Final Report

Project Title: Spatially Distributed Hydroecosystem Modeling of Everglades Ridge and Slough Landscapes

Project Number: J5284 08 0005

Abstract

A two-dimensional, spatially distributed flow dynamics model was developed and tested for a 1.5 by 4 km area of the patterned ridge and slough landscape of the Florida Everglades. This model is intended to support a deepened understanding of the system ecohydrological dynamics, and provide a useful tool for management decision support. The model was constructed with a fine enough mesh structure to ensure proper representation of ridge and slough topographic detail as well as capture local hydrologic influences. Upstream and downstream stage data collected near the study area in central Water Conservation Area-3A were used to establish the initial and boundary conditions. Water velocities measured in the ridges and sloughs over a three-year period were used to calibrate and verify the model. Hydraulic resistance was computed using a power-law relationship with water depth and different hydraulic resistance in the ridge and slough area was determined through model calibration. The simulated water levels, water depths, and flow velocities showed good agreement with the three-year field-monitored data with percent model errors of approximately 4%, 12%, and 10%, respectively. Computed differences in hydraulic resistance between ridge and slough were reduced significantly during the storm season compared to the dry season. This suggests that more solute and suspended solid mass can be redistributed from the sloughs to the ridges in particular during wet seasons, due to the weakened heterogeneity of hydraulic resistance during high flows. In addition, a Transport and Reaction Simulation Engine (TaRSE) was then coupled into the flow dynamic model for hypothesis testing on mass transport between ridge and slough. The example hypothesis examined here is that organic fine sediment can be transported from slough to adjacent ridge area and this mechanism contributes to maintenance of the topographic difference between ridge and slough area.

1. Introduction

Spatially distributed flow dynamics models can be used by aquatic ecosystem scientists and managers to help understand or predict hydrological, biogeochemical, or ecological changes over various time scales. In aquatic systems such as wetlands where key ecological processes are strong functions of the spatio-temporal changes in hydrodynamic parameters (i.e. water depth and flow velocity), integrating reactive transport models with ecosystem models enables testing of environmentally critical hypotheses through both hind- and forecasting scenarios. However, to obtain meaningful simulation or prediction results, one cannot overemphasize the importance of a robust flow dynamics model developed at a spatial scale consistent with the modeling purpose.

Human intervention to the Everglades during the last century has caused the loss of historic surface flow. The disturbed hydrology has been suspected as a trigger of the

partial loss of the unique ridge and slough landscape pattern in the central Everglades. Currently, temporal variation of hydrodynamic features in the remnant Everglades is mainly controlled by water management practices regulating flow (usually stormwater) from upstream hydraulic structures (Harvey et al., 2009). For the recent and proposed future restoration efforts, the role of surface water flow and organic-rich sediment (flocculent materials) transport as well as spatio-temporal change in hydroperiod has been highlighted due to the importance of physical and ecological impacts on the landscape formation, maintenance, and degradation (SCT, 2003; Leonard et al., 2006; Larsen et al., 2007, 2009; Noe et al., 2007). Restoring a more natural hydropattern and improving water quality in this ecosystem are critical components of the Comprehensive Everglades Restoration Plan (CERP) (Perry, 2004), including decompartmentalization – removal of canals and levees to restore the historic sheetflow through the remnant Everglades (i.e. to increase hydrologic connectivity of the system). While simple water balance models may be adequate for broad water resource management, a well developed flow dynamics model can play a foundational role in developing more advanced modeling tools to understand current hydrological and ecological effects on the wetland ecosystem and predict the future changes from the wetland ecosystem restoration.

Compared to recent systematic monitoring efforts on water flow and solute/particle transport in the patterned landscape of the Everglades (Saiers et al., 2003; Harvey et al., 2005b, 2008; Bazante et al., 2006; Leonard et al., 2006; Noe et al., 2007; Huang et al., 2008), physically based, spatially distributed modeling studies with local- or intermediate-scale (i.e. beyond pilot or mesocosm scales) have been rarely reported in this unique wetland ecosystem. The primary reason may be due to the difficulties in obtaining high resolution spatial data for model development (bathymetry, peat depth, vegetation type and density) and spatio-temporally distributed hydrologic data necessary for model setting, calibration, and validation, including field observations in both ridges and sloughs. Model grids in regional-scale models are too coarse to represent the topographic and vegetative heterogeneities effectively. The physical differences between ridges and sloughs form different flow characteristics. The average ponding depths, hydroperiods, flow velocities, and the transported water and solute fluxes are all different between the ridge and slough habitats (Noe and Childers, 2007). The different surface water flow characteristics regulate the formation and distribution of bimodal vegetative habitat, which impacts the flow again by creating different hydraulic resistances, ultimately controlling the landscape stability directly or indirectly.

The significance of heterogeneous topography and vegetation for understanding and modeling wetland flow characteristics have been well documented (Martinez and Wise, 2003; Dierberg et al., 2005; Jenkins and Greenway, 2005; Min and Wise, 2009). However, these impacts were not fully considered in previous spatially distributed regional modeling efforts for the bimodal ridge and slough landscape (SFWMD, 1994; Bolster and Saiers, 2002; SFWMDa, 2005) despite the acknowledged differences in hydrologic/hydraulic characteristics of ridges and sloughs. The objective of the present study was to examine the significance of topographic and the associated vegetative (in terms of hydraulic resistance) bimodality on the ridge and slough flow dynamics, which have not been considered in previous flow dynamics modeling efforts. The South Florida wetland ecosystem may be one of the best study areas in the world to develop

and test such a model due to decades of continuous and extensive hydrologic monitoring.

In this study, a two-dimensional (2-D), spatially distributed flow dynamics model was developed for the ridge and slough landscape and tested against hydrologic data, such as water level (*h*), depth (*d*), and flow velocity (*v*), collected from a typical ridge and slough area that is considered well-conserved. The modeling framework was the Regional Simulation Model (RSM) developed by the South Florida Water Management District (SFWMD) and a Transport and Reaction Simulation Engine (TaRSE) was then coupled into the flow dynamic model for hypothesis testing on mass transport between ridge and slough. The coupled RSM has been applied mainly for a large-scale (>10^3 km^2) basin with complex hydrology (Lal et al., 2005), but rarely used for relatively smaller-scale (~10 km^2) natural wetland systems. Hence, the second objective was to evaluate the usefulness of the RSM framework in predicting local- or intermediate-scale hydrology of the landscape accurately. The third objective was to evaluate the effect of limited spatial information on the ability to predict hydroperiods (seasonal pattern of water level in wetlands) and *v* in the Everglades ridge and slough landscape. The final objectives of the transport modeling study were to (1) understand the spatio-temporally different characteristics of mass transfer between ridges and sloughs using a spatially distributed transport modeling framework coupled with transient flow dynamics, (2) examine the ability of the model presented here for testing several hypotheses related to the role of flow and mass transport, and (3) elicit some implications for the restoration of ridge and slough landscape.

2. Site description

The selected model domain is a 1.5 by 4 km rectangle located approximately 4 km south of Alligator Alley (I-75) in Water Conservation Area 3A (WCA 3A, Fig. 1A and B). In this area the historic ridge and slough landscape pattern is considered to be well preserved (SCT, 2003; Harvey et al., 2009). The ratio of ridge and slough landscape is about 1:1 (Wu et al., 2006). Relatively higher-elevation ridge areas dominated by dense stands of sawgrass (*Cladium jamaicense*) have shallower *d* and shorter hydroperiod compared to adjacent lower-elevation sloughs, open water areas with plants accustomed to deeper *d*, such as *Nymphaea odorata*, *Eleocharis* spp., *Utricularia* spp., and *Panicum repens* (Fig. 1C). Jorczak (2006) reported that site J-1 located 2.4 km west of the model domain had an average topographic difference of 16 cm between ridge and slough and the difference increased toward downstream area of WCA 3A (elevation difference at the downstream area in Fig. 1B: 25 cm).

3. Methods

3.1. Modeling framework

3.1.1. RSM HSE

A physically based, spatially distributed numerical model for landscape flow dynamics was developed based on the Hydrologic Simulation Engine (HSE) of the SFWMD RSM. This finite volume based model was developed to comprehensively simulate various surface (overland flow in wetlands, hydraulic structure flow, and canal flow) and subsurface flows and their interactions principally for application to the complex regional hydrologic system of South Florida (Lal et al. 2005; SFWMD, 2007).

The HSE governing equations for mass and momentum conservation (St. Venant equations) are consistent with traditional surface flow dynamics models. The inertia terms of the momentum equation were neglected for diffusion flow assumption (Feng and Molz, 1997; Bolster and Saiers, 2002), which has been shown to be valid for most regional flows in the south Florida Everglades (Lal, 1998, 2000). The modified governing equations in integral form, based on Reynolds' transport theorem, are combined to generate a diffusion flow equation and solved using an implicit finite volume method. The model is implemented with two basic abstractions – "waterbodies" and "watermovers", which are used to represent the state within a control volume and the flux between the volumes, respectively (SFWMD, 2007). This allows multi-dimensional calculation of the storage in various waterbodies (overland, subsurface, canal and lake) and the flow between the waterbodies. Detailed descriptions of the RSM HSE modeling framework can be found elsewhere (Lal et al., 2005; SFWMD, 2005b, 2007).

3.1.2. RSM TaRSE

A mass transport model was developed based on the framework of RSM TaRSE (James and Jawitz, 2007) which was internally embedded with HSE of RSM. The RSM TaRSE is a linked-library model that runs with HSE which provides hydrologic information that is needed to simulate mass transport. RSM TaRSE is constructed in two parts: (1) transport (e.g., advection and dispersion) of solutes, and (2) a flexible biogeochemical reaction module. Information about topography, mesh, and run time step is controlled by the hydrologic model. For detailed information about RSM TaRSE discretization, boundary conditions, and numerical solution algorithms, the reader is referred to James and Jawitz (2007).

3.2. Hydrodynamic model setup

3.2.1. Model domain

The model domain size (1.5 km by 4 km) was selected to be large enough to capture the bimodal features typical of the ridge and slough landscape and yet small enough that model effectiveness would not be compromised by the number of calculations and the corresponding model running time. It was desired to employ a fine enough mesh structure to represent ridge and slough topographic detail, and the domain size was thus limited to approximately 10 km^2, rather than the approximately 10^3 km^2-scale of the entire hydrologic basin (WCA-3A). A 2004 Digital Ortho Quarter Quad (DOQQ) map of this study area and the selected model domain are illustrated in Fig. 2A. The rectangular model domain with the major axis parallel to the elongated ridge direction (i.e. main flow direction) comprises approximately four major ridges separated by three sloughs. No flow boundaries were assigned to the directions parallel to the main flow direction (Bolster and Saiers, 2002) as shown in Fig. 2B. The upper and lower boundaries were set based on long-term *h* data measured at nearby monitoring stations. The borders between the ridges and sloughs within the model domain followed the landscape boundary delineated by Cowardin et al (1979) (Fig. 2B) and there were no major discrepancies when compared to the recent pattern shown in the DOQQ map. For the model grid, an irregular triangular mesh, which is suitable to delineate the complex bimodal landscape boundaries, was generated with Groundwater

Modeling System (GMS) v5.1 (Brigham Young University, 2004) (Fig. 2C). The 2-D GMS mesh data file of the model domain is shown in Appendix A. The number of discretized grid cells was 962 (ridge: 486 and slough: 476). An enlarged portion of the model grid, shown in Fig. 2D, illustrates specific grid cell location of simulation output points for *d* and *v* at ridges (R1-3) and sloughs (S1-3), respectively. For comparison with the measurement data at J-1, these points were selected arbitrarily along the direction perpendicular to the main flow direction, considering the location of J-1. The simulation period was three years (January 1, 2002 to December 31, 2004) and the simulation time step was six hours.

3.2.2. Model bathymetry

The Everglades Depth Estimation Network (EDEN) is an active *h* and ground-elevation monitoring/modeling effort in the Everglades that enables scientists and managers to access current *h*, *d*, and topographic information (Chartier and Jones, 2007; Jones and Price, 2007; Pearlstine et al., 2007; Palaseanu and Pearlstine, 2008). However, the elevation model source data vertical resolution of ± 0.15 m and cross-validation error of 0.07 to 0.17 m (Chartier and Jones, 2007) were not sufficient to differentiate the subtle topographic difference between the ridges and sloughs (about 0.16 m) in the model domain. The average topographic difference between 14 EDEN DEM ridge points and 24 slough points was only 0.01 m ($p = 0.52$). Hence, the model bathymetry was constructed independently using available hydrologic monitoring data and geostatistical interpolation scheme and then confirmed with the EDEN data.

The average landscape slope was determined as follows. First, the upstream and downstream (see the locations in Fig. 1B) slough bottom elevations were estimated from the differences between 3 year average *h* at 3A-9 and *d* at CA311 and 3 year average *h* at 3A-4 and *d* at CA315: upstream/downstream slough 2.94/2.56 m NGVD29; slope = 0.0025%. With the assumption that the lateral bathymetric variation was negligible, a 2-D regional slough topographic map was created using spline interpolation method. The gently sloping landscape was set to be slightly steeper in the slough than the ridges according to the field observations of Jorczak (2006). Ridge bottom elevations were estimated by adding topographic differences measured by Jorczak (2006) in the upstream and downstream areas (0.16 and 0.25 m) to the slough bathymetry estimates: upstream/downstream ridge 3.10/2.81 m NGVD29; slope = 0.0019%. A regional ridge map was made using the same interpolation scheme. These two regional maps were cut along the ridge and slough boundary and merged into a final bathymetry map using ArcGIS 9.2, illustrated in Fig. 2E. The upper/lower boundary ridge and slough topographic elevations were determined to be 3.10 and 2.94 m/3.02 and 2.84 m, respectively. The average ridge topographic elevation over the entire model domain (3.06 ± 0.02 m) was 0.17 m greater than in sloughs (2.89 ± 0.03 m), generating topographic differences between the bimodal landscapes that increased from 0.16 to 0.18 m along the main flow direction. These ridge/slough topographic differences are very close to the average difference (0.15 m) reported by Givnish et al. (2008) across the study regions (WCA-3A/3B). Differences between the calculated slough bathymetry and the EDEN DEM data near the model boundaries were only 0.03 to 0.05 m. Also, the estimated regional topographic slope of 0.0025% was comparable to those reported by

Kushlan (1990; 0.0030%) and Harvey et al. (2009; 0.0033%). Peat soil depth of 0.8 m was assumed to be constant throughout the entire model domain (Jorczak, 2006).

3.2.3. Boundary and initial conditions

In systems with intensive hydraulic manipulation, such as the Florida Everglades, local processes such as rainfall and ET may not be sufficient to predict local hydrologic response. The hydrodynamic simulations of Bolster and Saiers (2002) were more sensitive to the upstream boundary conditions than rainfall or ET. Here, daily averaged *h* measured at 3A-9 were used for the upper boundary during the simulation period and the lower boundary was set through linear interpolation between *h* measured at 3A-9 and at 3A-4. This lower boundary was consistent with the average *h* measured at nearby EDEN monitoring stations (average difference 0.01 to 0.03 m). For the initial *h* condition, the average *h* value (3.32 m) of the upper and lower ones measured on the simulation starting date (January 1, 2002) was assigned throughout the model domain. The specific model input conditions incorporated in RSM HSE are shown in Appendix B.

3.2.4. Hydrologic data

To develop and test a 2-D, spatially distributed flow dynamics model, hydrometeorological data collected from the central portion of WCA 3A were used. Spatially uniform rates of daily based rainfall and potential ET (PET) were applied throughout the entire model domain. Daily based rainfall and PET data were collected by SFWMD at 3A-S and S140, respectively (Fig. 1B). Approximately 10% missing values in the S140 PET data during the simulation period were substituted with PET measured at 3AS3WX, a monitoring station located in the southern WCA-3A (the median value of absolute differences between the remnant comparable PET data monitored at these two stations was 0.38 mm; correlation coefficient = 0.79). These data are publically available through the SFWMD online database, DBHYDRO (http://my.sfwmd.gov/dbhydroplsql/show_dbkey_info.main_menu). Actual ET was calculated using the ET crop correction coefficient (K_c) which was determined as a function of *h* (SFWMD, 2005b). When *h* was greater than the ponding depth (fixed to 2.0 m in this study, considering the maximum height of sawgrass), K_c = 1.0 (open water condition). The K_c value linearly decreased as *h* decreased to the ground surface (d = 0). When d = 0, the K_c value corresponded to the root zone ET coefficient (K_{veg}). To assign the temporally variable K_{veg} values, the monthly averaged values (0.88 ± 0.05) calibrated in South Florida Water Management Model (SFWMM) v5.5 for sawgrass plains (SFWMD, 2005a) were used in this study. When *h* was in the shallow root zone (top 0.5 m of soil), $K_c = K_{veg}$ and then again the K_c value was linearly decreased from the point d = -0.5 m to the extinction depth (fixed to a depth of 1 m below ground surface) where K_c = 0. In this modeling study, the K_{veg} coefficients were assumed to be homogeneous regardless of the ridges and sloughs due to the lack of reliable information at finer scales.

Long-term hydrologic data, such as *h*, *d*, and *v*, monitored around the study area were also used for model setup and testing. Daily averaged *h* and biweekly measured *d* data were monitored by SFWMD or USGS (available from EDEN: http://sofia.usgs.gov/eden/) at the locations shown in Fig. 1B. Jorczak (2006)

independently measured *v* (and *d*) at the ridge and slough site of J-1 over a period of 16 months (November 2002 to February 2004).

Groundwater-surface water interaction was not modeled in this study because groundwater exchanges determined by Harvey et al. (2004 and 2005a) in WCA-3A (Site 3A-15, near our study site) were the smallest in the central Everglades. These authors concluded that the interior area of WCA-3A (our study area), which is far from levees and canals, may be the best modern analog for pre-drainage conditions with net groundwater exchange <1% (Harvey and McCormick, 2009). This is in contrast to the present-day managed condition of the central Everglades that is heavily influenced by drainage and control structures with net groundwater recharge as high as 16% (Harvey and McCormick, 2009).

Wind effects were also not included in this study. Although wind sometimes plays an important role in solute transport in shallow aquatic bodies (Langevin et al., 2005; Swain, 2005), this impact can be minimized in densely vegetated wetlands like the sawgrass ridges since the emergent vegetation dampens wave energy and shelters the water surface from wind stress (Nepf, 1999; Braskerud, 2001). Also, submerged aquatic vegetation such as found in sloughs has been reported to be effective in limiting wind-driven sediment/nutrient resuspension (Barko and James, 1997; Horppila and Nurminen, 2003). Therefore, wind effects were considered to be relatively less dominant compared to gravitational forces in controlling flow in the low gradient, patterned bimodal landscape.

3.2.5. Model calibration: hydraulic resistance

A general power law form of frictional equations used for overland flow in wetlands was suggested by Kadlec and Knight (1996):

$$v = ad^{b-1}S^{c} \qquad (1)$$

where *v*, *d*, and *S* are surface water flow velocity, water depth, and water surface slope, respectively. For the friction parameters (*a*, *b*, and *c*), Kadlec and Knight (1996) recommended $a = 10^7/5\times10^7$ $m^{-1}d^{-1}$ (densely/sparsely vegetated), $b = 3.0$, and $c = 1.0$ (Table 1). Also, Bolster and Saiers (2002) estimated $a = 5.1\times10^6$ $m^{0.46}d^{-1}$, $b = 1.54$, and $c = 1.0$ through model calibration to *h* measured at Shark River Slough (Table 1). Eq. 1 is equivalent to Manning's equation when $a = 1/n$, $b = 1.67$, and $c = 0.5$. The Manning's roughness coefficient, *n*, has been widely used to represent a lumped hydraulic resistance in wetlands in spite of the theoretical inappropriateness indicated by Kadlec and Knight (1996). Considering a general trend that Manning's *n* decreases as *d* increases (Kadlec and Knight, 1996), SFWMD (1994; 2005a, b) suggested an empirical relationship between Manning's *n* and *d* as follow:

$$n = Ad^{B} \qquad (2)$$

where the empirical coefficients, *A* and *B*, are usually determined through model calibration. The magnitudes of *A* and *B* probably depend on wetland habitat (vegetation type) or vegetation density (given a wetland type) and the vertically nonlinear characteristics of a *d*-dependent resistance curve (i.e., given a wetland type, a vertical *v* profile), respectively. According to SFWMD (1994, 2005a), the value of $B = -0.77$ was satisfactory in most wetland habitats. Hence, a modified Manning's equation with the relationship of Eq. 2 can be arranged as:

$$v = \frac{1}{Ad^{-0.77}} d^{0.67} S^{0.5} \qquad (3)$$

In this framework, a spatio-temporally variable Manning's *n* is determined from the calculated *d* at each grid cell every simulation time step. This *d*-dependent Manning's equation cannot be directly expressed in the form of Eq. 1 because *a* would not be temporally constant.

We tested the above cases through model calibration of the resistance parameters, *a* or *A*, to measured *v* and *h* profiles at the ridge and slough area, respectively (Table 1). Uniform vegetation density within each bimodal habitat was assumed in this study due to the lack of spatial distribution data in vegetative cover. A surface water detention depth of 0.03 m was assigned over the model domain, below which no flow occurred even if a hydraulic gradient was calculated (Appendix B).

3.3. Transport model setup

The transport algorithm of RSM TaRSE was used to simulate 2-D transport of arbitrary mass in the ridges and sloughs. It was designed to simulate water quality conditions and ecosystem responses to hydrologic and water management changes in wetland environments. RSM TaRSE simulates conservative/reactive transport of mobile materials in variable-depth water bodies, and numerically solves the advection-dispersion-reaction equation. The accuracy of the model was determined by comparing analytical solutions with simulations in one and two-dimensions with non-reactive and reactive transport (James and Jawitz, 2007). Here, the model is used to simulate 2-D non-reactive transport in a field-scale wetland with variable depth flow. Examples of the transport model xml input files (RSM HSE & TaRSE) are attached in Appendices C and D, which show a case of transport simulation on dry season under current flow regime.

3.3.1. Simulated tracer transport

Based on the developed flow dynamic model setting, two different transport simulations (dry and wet period) were carried out. An arbitrary concentration of a conservative mass was injected at an upstream slough grid cell and the generated plume distribution and mass transfer rate in the downstream grid cells were compared seasonally as shown in Fig. 3. For dry season transport simulation, a conservative mass of 30 kg was injected on March 1, 2002 and the transport at the downstream points was monitored during the period of a month. The simulation time step was 10 minutes and was based on the real time hydrology (measured upper and lower boundaries). During the period, the average water depth and flow velocity at the tracer injection slough grid cell (asterisk in Fig. 3) were 0.29 m and 0.4 cm/s, respectively. Likewise, the same amount of mass was injected at the same point on August 1, 2002 for wet season transport simulation. The only difference from the dry season case was the hydrodynamic condition of the system – a much deeper water depth (0.62 m) and doubled flow velocity (0.8 cm/s). In these simulated tracer tests, rainfall and ET were excluded in the model because the main concern was to compare the seasonal difference in mass transfer from slough to ridge, not to mimic the temporal hydrology.

3.3.2. Dispersivities

Under the coupled modeling framework, longitudinal and transverse dispersivities [L] should be determined to describe the dispersive characteristics of mass transport. In this study, longitudinal and transverse dispersivities were set at 20 m and 2 m (Table 2), respectively, considering the values reported from literature (Ho et al., 2009; Min et al., 2010; Paudel et al., 2010). In particular, the average dispersion coefficient values calculated with these dispersivities were within the range suggested by Ho et al. (2009), which was reported for a similar ridge and slough area.

3.3.3. Cases of restored flow regime

This model was also used to examine mass transport under restored flow regime (faster flow and deeper water depth generated by increasing water level (+0.2 m) of model boundaries) in addition to current flow regime. According to Larsen et al. (2007 and 2009), faster flow velocity than current flow regime was required to facilitate sediment redistribution from slough to ridge. Although the constant increasing of water level by 20 cm may not be enough to represent the restored flow regime (no study is available for the pattern and extent of restored flow regime), it was used here to represent the suggested restored flow regime (faster flow and deeper depth). Hence, additional model validations on the restored flow regime are needed in the future. The transport model setup was the same with the dry and wet simulation cases under current flow regime except the upper boundary condition, which was raised by 20 cm from the measured water level profile. It caused faster flow velocities and deeper water depths as summarized in Table 2.

4. Results

4.1. Hydrodynamic modeling

The ridge and slough *v* profiles measured at J-1 were compared to daily average simulated *v* profiles at R1-3 and S1-3. The model calibration process was not finalized until the RMSE between the measured *v* (N = 7) and the averaged value of *v* simulated at the three points was minimized. First, the values recommended by Kadlec and Knight (1996) and estimated by Bolster and Saiers (2002) were tested, but the results were not satisfactory (Table 1). Subsequently, the resistance parameters, a or A, were estimated by model fitting with the other parameters fixed: (1) Kadlec type: a = calibration parameter, b = 3.0 and c = 1.0, (2) Modified Manning: A = calibration parameter, b = 1.67 and c = 0.5, (3) Manning: a ($1/n$) = calibration parameter, b = 1.67 and c = 0.5. As summarized in Table 1, the *v* model calibration results reveal that the average RMSE was lowest when the modified Manning's equation was used. For ridge *v*, the RMSE was lowest (0.139 cm/s) when A = 0.19 (R^2 = 0.86). For slough *v* the RMSE was lowest (0.143 cm/s) when A = 0.17 (R^2 = 0.90). Also note that the model calibration to *h* was much less sensitive compared to the *v* model calibration (Table 1). For hydraulic resistance in this study, depth-dependent Manning's approach (A = 0.19 (ridge) / 0.17 (slough), b = 1.67, and c = 0.5) was therefore applied to each ridge and slough finite element at each simulation time step. This was also supported by comparison to other common metrics of model performance: R^2, Bias, and Nash-Sutcliffe model efficiency coefficient (N-S) (Table 1). Although the field *v* observations were limited (e.g., there was only one wet season field measurement), the model predicted the temporal fluctuation and spatial difference of each *v* profile in the bimodal landscape reasonably

(discussed further below). More systematic flow velocity data collection efforts (at least nine monitoring stations longitudinally and transversely – three by three in future monitoring efforts) are necessary to reduce the uncertainties associated with the low frequency of observations and confirm the calibration accuracy.

4.1.1. Spatio-temporal variation of hydraulic head

Daily averaged *h* and biweekly measured *d* were monitored by USGS and SFWMD at the two interior slough points of the model domain (3A-S and CA311). Hydraulic heads simulated at the corresponding model grid cells were compared to the field measurements (Table 3). The average *d* (±1 SD) measured at CA311 (slough) and simulated at the corresponding grid cell (see the location in Fig. 2D) were 0.43 ± 0.20 m and 0.41 ± 0.19 m, respectively ($p = 0.36$). Fig. 4 also shows that the simulated hydraulic heads closely match the spatial and temporal variations in field observations for three years. Simulation error for *d* ($R^2 = 0.74$; RMSE = 0.09 m) was greater than for *h* ($R^2 = 0.98$; RMSE = 0.04 m). This is likely due to the higher uncertainties of manually measured *d* including the local difference of microtopography (Sutron Corp., 2004). The percent model errors (PME), defined as RMSE divided by the range of the measured data, were about 4 and 12% for *h* and *d*, respectively. Conrads and Roehl (2007) reported PME less than 6% for estimating *h* at 25 new Everglades gauging stations using EDEN. Our hydraulic head simulation RMSE (0.04 m) was slightly higher than the EDEN water surface model RMSE (about 0.025 m) in WCA-3A reported by Violin et al. (2008).

The average (± 1 SD) *d* (N = 6) monitored by Jorczak (2006) in both the ridge (0.23 m ± 0.10 m) and slough (0.39 m ± 0.10 m) of J-1 were compared to averages of the daily based *d* simulated at R1, 2, 3 (0.27 m ± 0.16 m) and S1, 2, 3 (0.44 m ± 0.16 m) (see the specific grid cell location in Fig. 2D) during the same time period. These simulation output points were selected arbitrarily along the direction perpendicular to the main flow direction based on the location of station J-1. The topographic and hydrologic conditions at J-1 were assumed to be similar to those at the R1-3/S1-3. The average simulated *d* values were slightly higher than the measured values (0.04 to 0.05 m on average).

4.1.2. Hydroperiod

Hydroperiod plays a key role on vegetation dynamics and the biogeochemistry of organic rich soil in wetland ecosystems; thus, it is important to accurately predict the spatio-temporal pattern of this parameter in ecohydrological modeling efforts (Townsend, 2001). The simulated three-year *d* at R1-3/S1-3 were used to calculate ridge and slough hydroperiods in the study area. For the slough, there were no days when *d* was less than 0.01 m (i.e. 100% hydroperiod under current flow regime controlling the *h* boundaries). The ridge was dry for less than one month per year (6%), with $d < 0.01$ m 9% of the time, for ridge and slough hydroperiod of 91 to 94%. The spatio-temporal extent of hydroperiod simulated in this study is very close to the general patterns reported by other investigators in multiple locations of the patterned landscape (Ross et al., 2006; Givnish et al., 2008), which also supports appropriateness of the model setting based on the limited spatial data.

4.1.3. Flow velocity

The best model fits to the *v* profiles measured by Jorczak (2006) at site J-1 are shown in Fig. 5. Note the several intermittent discrepancies in correlation between rainfall and flow velocity peaks denoted in Fig. 5, highlighting the importance of upstream water management practices in controlling the regional hydrology (Harvey et al., 2009). Although the current flow regime does not fully follow the historic rainfall-driven sheetflow pattern, the temporally fluctuating hydrologic pattern is still distinct as shown in the field observations of hydraulic head and *v* (Figs. 4 and 5). During the dry season (November to May), the modeled *v* did not usually exceed 0.5 cm/s in either ridges or sloughs. In the wet season (June to October) *v* was much faster, with short-duration peaks greater than 2 cm/s in sloughs (Fig. 5). Although the pattern of seasonal variation of simulated *v* was well captured, additional wet-season v measurements are needed to confirm the magnitudes of predicted wet season *v*. Note that Harvey et al. (2009) reported seasonal ranges of measured *v* of 0.02 to 0.79 cm/s. Typical snapshots of dry and wet season simulated flow pattern are illustrated in Fig. 6. In addition to the overall trend of faster/sluggish velocities in the wet/dry seasons, *v* was always higher in sloughs compared to adjacent ridges. The simulated three year average *v* at the three slough grid cells (S1-3) was approximately 40% higher than at the ridge cells (R1-3) (Table 4). These results are consistent with long term field measurements reported by Harvey et al. (2009), that average ambient *v* measured in central WCA-3A were typically on the order of 0.3 cm/s and the average *v* was 29% higher in sloughs compared to ridges over a three year monitoring period.

4.1.4. Hydraulic resistance

Several types of frictional equations (Manning's and Kadlec-type) were tested in this study. Direct use of previously reported parameter values for the general form of the wetland flow frictional equation was not suitable in simulating *v* in the ridge and slough area (Table 1). When calibrated to *v* measured in the study area, the simulation results with modified Manning's approach were slightly better than those of Kadlec-type and traditional Manning's approach (Table 1). Also, compared to *v*, *h* was not sensitive to the friction parameters (Table 1). This may be related to setting the boundary condition based on *h*. Hence, for models assigned by *h* boundaries, using *h* may be inappropriate to calibrate the hydraulic resistance.

Manning's roughness coefficients (*n*) were determined for ridges and sloughs as a function of *d* using Eq. 2 and the model-calibrated hydraulic resistance parameter, *A* (Fig. 7A). For the three year averaged *d* simulated at the model grid corresponding to CA311 (ridge: 0.24 m and slough: 0.41 m), Manning's *n* values of 0.57 and 0.34 $s/m^{1/3}$ were calculated for the ridges and sloughs, respectively. During the wet season, as *d* increased, the lumped hydraulic resistances were reduced to 0.42 and 0.28 $s/m^{1/3}$, respectively. During the dry season, the shallow *d* increased the roughness coefficients to 0.81 and 0.41 $s/m^{1/3}$.

The average Manning's roughness coefficient values calculated here were compared to the values calibrated in various south Florida landuse patterns under the same hydraulic resistance modeling framework, SFWMM v5.5. For the central/southern WCA-3A wetland area (categorized as "Ridge and Slough II" in SFWMM), which includes the model domain of this study, the average ridge and slough Manning's

values were 0.62 and 0.41 s/m$^{1/3}$ (A = 1.25/B = -0.77 SFWMD, 2005a). These estimates were close to those determined in this study (ridge: 0.57 and slough: 0.34 s/m$^{1/3}$). In addition, those values were 3 to 5 times greater than the n values (ridge: 0.13 and slough: 0.11 s/m$^{1/3}$) calibrated with traditional Manning's equation (Table 1). This shows that a simple application of model-calibrated constant Manning's n in wetlands with highly transient flow regime should be done with caution because it may cause a significant underestimation of hydraulic resistance, particularly during dry seasons.

To evaluate the impact of change in topographic slope on the relationship between d and Manning's coefficients, only the model topographic slope was doubled/halved under the same model condition and then the non-linear relationships were reconstructed (Fig. 7B). This figure shows that if the topographic slope of study area were steepened/flattened twice, the hydraulic resistances estimated here should be increased/decreased by about 40%/30%, respectively.

4.1.5. Sensitivity test

Sensitivity test results of model-calculated v profiles to changes in the empirical hydraulic resistance coefficient, A (±30%) are illustrated in Fig. 4. The sensitivity of v to the changes in A was evaluated using the sensitivity coefficient $S_{v,A} = \frac{\Delta v / v}{\Delta A / A}$. For example, a sensitivity coefficient of -0.5 indicates that a 10% increase of A would decrease v by 5%. Table 4 shows the resulting A values, RMSEs, and sensitivity coefficients. When the model-calibrated coefficient values were increased/decreased by 30% in the ridges and sloughs simultaneously, three year-averaged v simulated in the bimodal landscape (R1-3/S1-3) decreased/increased by approximately 22%/40%.

4.2. Transport modeling

4.2.1. 2-D tracer plume and BTC

For the four different hydraulic cases (current dry, current wet, restored dry, and restored wet flow regime) proposed above, 2-D mass transport modeling results are shown in Figs. 8 and 9. The generated shape of 2-D tracer plumes is largely affected by the hydraulic condition summarized in Table 2. For instance, the highest concentration in current dry flow regime (red color as denoted in Fig. 8a) illustrates relatively long hydraulic retention time due to the lowest flow velocity; conversely, the lowest level in restored wet flow regime indicates that most of injected mass was transported far downstream within the monitored time frame (1 month). Fig. 9 shows the BTCs of each case. At both current and restored flow regime, the shape of BTCs at downstream ridges and sloughs in wet seasons is more similar than those in dry seasons in terms of time to peak and the degree of spreading of the curves. This shows that hydraulic heterogeneity of the bimodal landscape is reinforced during the dry season. In other words, mass transfer between ridges and sloughs is more limited in the dry season.

4.2.2. Mass transfer between ridges and sloughs

Calculated mass transfer rates between ridges and sloughs located at the downstream side of tracer injection point are shown in Fig. 8. Under all flow regimes evaluated here, sloughs are the dominant pathway of flow-driven mass (>70%), but more mass was distributed from upstream slough grid cells into the right downstream

ridge grid cells during wet seasons. The seasonal differences were about 10% and 5% in current and restored flow regime, respectively. This result supports the implication from the temporal variation of estimated hydraulic resistance (Fig. 7a) that more uniform hydraulic resistance in the ridge and slough areas during the wet season is favorable to mass transfer between ridges and sloughs. Also, mass transport from the downstream slough to ridge was about four to six times higher at the head of elongated ridge than at the side of ridge. This elevated mass transfer at the head of ridges supports the significance of flow and sediment transport in regulating the formation, growth, and degradation of elongated ridges in this bimodal landscape. It is noted that the instantaneous tracer injection testing used in this study is not enough to quantitatively assess the patterned landscape formation and degradation. Finally, the impact of hydrologic restoration was higher in the dry season (more mass transfer by 8%) than in the wet season (by 3%).

5. Discussion

5.1. Hydraulic resistance modeling in the patterned wetlands

In view of traditional open channel hydraulics, the Manning's coefficient (*d*-independent, constant *n*) has been primarily focused on frictional resistance due to drag by a channel bottom; however, the hydraulic resistance on surface flow in vegetation-covered wetlands is predominantly dependent on the depth-specific vegetation stem/litter density and morphology (Kadlec, 1990; Kadlec and Knight, 1996; Nepf, 1999; Lightbody and Nepf, 2006). The nonlinear relationship between *d* and lumped hydraulic resistance used in this study was based on the assumption of high resistance for shallow flow due to high stem density, undergrowth and non-decomposed organic debris (litter) near the ground surface. In this framework, it is similarly assumed that flow resistance decreases with flow depth. However, some previous observations have not fully supported the exponential relationship between resistance and ponding depth. For example, Lightbody and Nepf (2006) reported that in a Massachusetts *Spartina alterniflora* salt marsh, vegetation volumetric frontal area and *v* are maximal and minimal, respectively, near 0.10 m from the bed, not the bottom elevation, but above the critical *d*, stem density decreased exponentially. Also, Schaffranek et al. (2003) reported vertically constant *v* profiles above around 0.10 m from the bed in an unburned, medium dense sawgrass area in Everglades National Park and an approximately linear increase of *v* with *d* at a burned, sparsely dense site.

In this study, the empirical approach shown in Eq. 2 was used under the assumption that the modified Manning's coefficient represented the overall lumped depth-variable resistance exerted by the ridge and slough vegetation as well as the sediment layer. The method employed here is consistent with the form suggested by Kadlec and Knight (1996) and applied by Bolster and Saiers (2002) and Kazezyilmaz-Alhan et al. (2007), with the notable difference that the resistance parameter, *a*, is expressed as a range rather than a constant (Table 1). The power-law relationship between *d* and hydraulic resistance resulted in the lowest RMSE (Table 1) compared to measured *v* profiles in ridges and sloughs, and provided values consistent with previous regional modeling efforts in the Everglades (SFWMD 1994, 2005a).

Accurately modeling vegetative cover hydraulic resistance in wetlands is one of the most challenging topics in wetland flow dynamics modeling. Vegetation cover and

associated hydraulic resistance changes horizontally, vertically, and temporally as a function of many factors, such as vegetation type, density, and morphology, and wind. A more complex mathematical description of the spatio-temporal variation of hydraulic resistance in wetlands would contribute to accurately simulating the complex natural phenomena, but may also increase the complexity of numerical models and decrease the ease of model application, requiring additional, systematic field surveys (Bolster and Saiers, 2002). Therefore, it is suggested that future improvements in hydraulic resistance modeling efforts in these patterned wetlands should be based on higher density spatio-temporal field measurements of *v* and vegetation community characteristics in both ridges and sloughs.

5.2. Hydrodynamic model implication on the mass redistribution

It has recently been acknowledged that flow and mass transport play a critical role in the formation, maintenance, and degradation of the Everglades ridge and slough landscape (SCT, 2003; Ross et al., 2006; Larsen et al., 2007; Larsen et al., 2009). Despite recent monitoring efforts on the characteristics of organic rich sediment and critical *v* regulating sedimentation and resuspension in water column, our understanding of the flow dynamics and mass transport is still limited in this unique wetland ecosystem.

The calculated relationships between *d* and Manning's *n* (Fig. 7A) indicate a significant seasonal difference in hydraulic resistance for the ridges and sloughs. The average difference of the lumped coefficient between ridges and sloughs was 0.14 as a Manning's coefficient unit during the wet season. However, this difference was nearly tripled (0.40) during the dry season (Fig. 7A). This phenomenon is even more pronounced over shorter durations. For example, in one of driest months, April, the three year average difference (1.11) was almost an order of magnitude higher than the average difference on August (0.12). The average slough to ridge *v* ratio was 1.9 in April, but only 1.4 in August.

One may conclude that such differences in the depth-dependent hydraulic resistance relationships between the ridges and sloughs are not significant, and that the separation into a bimodal landscape is not necessary in terms of hydraulic resistance. However, it is emphasized that the utility of this discretization is fully dependent on the modeling purpose. For long term, regional scale water management, a single hydraulic resistance value relationship is likely sufficient. However, the subtle seasonal differences in velocity between ridge and slough may be of overriding importance in developing and applying a hydro-ecosystem model to simulate mass transport and peat accretion processes that may be different between ridges and sloughs.

Temporally variable characteristics of hydraulic resistance between ridges and sloughs are likely to regulate the interconnectivity of mass transport between these habitats. Ridges may act as barriers to flow and mass transfer during the dry season, but the degree of restriction is likely to be significantly reduced during wet seasons. In view of sediment redistribution between ridges and sloughs, the smaller wet season difference of flow resistance between ridges and sloughs and faster *v* conditions are favorable for floc entrainment, increased allochtonous sediment input and greater transport of organic-rich particles from sloughs to ridges that eventually accumulate due to the relatively shallower *d* and slower *v*. Larsen et al. (2009) hypothesized that net transport of organic floc from open to vegetated areas during high flows is critical for

forming and maintaining the patterned landscape in the Everglades. This study shows that the weakened heterogeneity in hydraulic resistance in the bimodal landscape during high flows facilitates such mass redistribution.

5.3. Transport model implication on the mass redistribution

The best fit model values of depth-dependent Manning's coefficient to each flow velocity profile measured at ridge and slough zone showed that there was a significant seasonal difference of hydraulic resistance in the bimodal landscape. Temporally different characteristics of hydraulic resistance in ridge and slough area regulated the interconnectivity of mass transport between the bimodal landscape. Ridges may act as barriers to flow and solutes/particles in the dry season but the degree may be significantly reduced in the wet season (Fig. 7a). For sediment redistribution, organic-rich particles may be transported from sloughs and accumulated into ridges due to the shallower water depth and slower flow velocity (easier to be trapped/deposited) in ridges during the dry season and the less flow resistance in the wet season. Mass transport from the downstream slough to ridge was about four to six times higher at the head of elongated ridge than at the side of the ridges. Also the impact of hydrologic restoration was higher in the dry season than in the wet season. As shown in Table 2 and Fig. 5, the simulated average flow velocity was generally less than recently reported values (2-5 cm/s) on critical flow velocity to cause floc resuspension in both current and restored flow regimes (current water level + 0.2 m). This shows that flow velocity, which is fast enough to exceed the threshold values, may not be dominant except during severe storm event periods even under a restored flow regime. Filtration of fine particles by vegetation and resuspension into the water column will be incorporated into the model with long-term continuous injection scenarios, which will help quantitatively understand the impacts of peat accretion due to allogenic sediment transport and autogenic sediment storage in ridge and slough area.

6. Summary and Conclusions

Despite the simplifying assumptions of uniform rainfall and ET, linear topographic slope and uniform vegetation density within each bimodal habitat, and a power-law relationship between *d* and hydraulic resistance, the simulated *h*, *d*, and *v* showed good agreement with the three-year field-monitored data. Our simulation results also suggest that the RSM HSE can be used to accurately predict the relatively smaller-scale hydrology of the patterned wetland area in the Everglades. Temporally averaged Manning's *n* values of 0.57 and 0.34 $s/m^{1/3}$ were obtained through model calibration for the ridge and slough zones, respectively. According to the *d*-dependent hydraulic resistance relationship, the ridge and slough hydraulic resistance differences were reduced significantly during the storm season compared to the dry season. This result supports a hypothesis that more dissolved or suspended mass transported from the upstream slough or resuspended from the slough bottom can be redistributed into the ridge area, in particular during wet seasons, due to the weakened heterogeneity of hydraulic resistance during high flows.

The flow dynamics model developed here ultimately can be linked with an optimized ecosystem model to determine key mechanisms of landscape degradation and evaluate restoration scenarios. For this, more systematic field monitoring efforts on

the depth-specific *v* and vegetation stem/litter densities as well as hydroperiod in the ridges and sloughs are required to confirm the values and hypothesis suggested in this modeling study. For example, development of more advanced ridge and slough coupled flow dynamics and ecosystem models that allow simulation of ecohydrological and biogeochemical feedbacks may require finer horizontal and vertical resolution spatial data, perhaps to the level of grid cell used in this study.

References

Barko, J.W., James, W.F., 1997. Effects of submerged aquatic macrophytes on nutrient dynamics, sedimentation, and resuspension. In: The structuring role of submerged macrophytes in lakes – Ecological studies 131, Jeppesen et al. (Eds.), Springer, New York, 197–214.

Bazante, J., Jacobi, G., Solo-Gabriele, H.M., Reed, D., Mitchell-Bruker, S., Childers, D.L., Leonard, L., Ross, M., 2006. Hydrologic measurements and implications for tree island formation within Everglades National Park. Journal of Hydrology 329, 606–619.

Bolster, C.H., Saiers, J.E., 2002. Development and evaluation of a mathematical model for surface water flow within the Shark River Slough of the Florida Everglades. Journal of Hydrology 259, 221–235.

Braskerud, B.C., 2001. The influence of vegetation on sedimentation and resuspension of soil particles in small constructed wetlands. Journal of Environmental Quality 30, 1447–1457.

Brigham Young University, 2004. The Department of Defense Groundwater Modeling System, GMS v5.1, Environmental Modeling Laboratory.

Chartier, K., Jones, J., 2007. Everglades Depth Estimation Network (EDEN) November 2007 digital elevation model for use with EDENapps. USGS. Available from: <http://sofia.usgs.gov/metadata/sflwww/eden_dem_cm_nov07_nc.html>.

Conrads, P.A., Roehl, E.A., Jr., 2007. Hydrologic record extension of water-level data in the Everglades Depth Estimation Network (EDEN) using artificial neural network models, 2000-2006. USGS Open-file report 2007-1350, 56 p. Available from: <http://pubs.water.usgs.gov/ofr2007-1350>.

Cowardin, L.M., Carter, V., Golet, F.C., LaRoe, E.T., 1979. Classification of wetlands and deepwater habitats of the United States. US DOI, Fish and Wildlife Service, Washington, DC. FWS/OBS-79/31.

Dierberg, F.E., Juston, J.J., DeBusk, T.A., Pietro, K., Gu, B.H., 2005. Relationship between hydraulic efficiency and phosphorus removal in a submerged aquatic vegetation-dominated treatment wetland. Ecological Engineering 25, 9–23.

Feng, K., Molz, F.J., 1997. A 2-D, diffusion-based, wetland flow model. Journal of Hydrology 196, 230–250.

Givnish, T.J., Volin, J.C., Owen, V.D., Volin, V.C., Muss, J.D., Glaser, P.H., 2008. Vegetation differentiation in the patterned landscape of the central Everglades: importance of local and landscape drivers. Global Ecology and Biogeography 17, 384–402.

Harvey, J.W., Krupa, S.L., Krest, J.M., 2004. Ground water recharge and discharge in the Central Everglades. Ground Water 42 (7), 1090–1102.

Harvey, J.W., McCormick, P.V., 2009. Groundwater's significance to changing hydrology, water chemistry, and biological communities of a floodplain ecosystem, Everglades, South Florida, USA. Hydrogeology Journal 17, 185–201.
Harvey, J.W., Newlin, J.T., Krest, J.M., Choi, J., Nemeth, E.A., Krupa, S.L., 2005a. Surface-water and ground-water interactions in the Central Everglades, Florida. USGS Scientific Investigation Report 2004-5069.
Harvey, J.W., Saiers, J.E., Newlin, J.T., 2005b. Solute transport and storage mechanisms in wetlands of the Everglades, south Florida. Water Resources Research 41, W05009, doi:10.1029/2004WR003507.
Harvey, J.W., Schaffranek, R.W., Noe, G.B., Larsen, L.G., Nowacki, D.J., O'Connor, B.L., 2009. Hydroecological factors governing surface water flow on a low-gradient floodplain. Water Resources Research 45, W03421, doi:10.1029/2008WR007129.
Ho, D.T., Engel, V.C., Variano, E.A., Schieder, P.J., Condon, M.E., 2009. Tracer studies of sheet flow in the Florida Everglades. Geophysical Research Letter 36, L09401, doi:10.1029/2009GL037355.
Horppila, J., Nurminen, L., 2003. Effects of submerged macrophytes on sediment resuspension and internal phosphorus loading in Lake Hiidenvesi (southern Finland). Water Research 37, 4468–4474.
Huang, Y.H., Saiers, J.E., Harvey, J.W., Noe, G.B., Mylon, S., 2008. Advection, dispersion, and filtration of fine particles within emergent vegetation of the Florida Everglades. Water Resources Research 44, W04408, doi:10.1029/2007WR006290.
James, A.I., Jawitz, J.W., 2007. Modeling two-dimensional reactive transport using a Godunov-mixed finite element method. Journal of Hydrology 338, 28–41.
Jenkins, G.A., Greenway, M., 2005. The hydraulic efficiency of fringing versus banded vegetation in constructed wetlands. Ecological Engineering 25 (1), 61–72.
Jones, J.W., Price, S.D., 2007. Everglades Depth Estimation Network (EDEN) digital elevation model research and development. USGS Open-file report 2007-1034, 29 p.
Jorczak, E., 2006. Influence of hydrology on Everglades ridge and slough soil topography. M.S. Thesis, University of Florida, Gainesville, FL.
Kadlec, R.H., 1990. Overland flow in wetlands: vegetation resistance. Journal of Hydraulic Engineering 116 (5), 691–706.
Kadlec, R.H., Knight, R.L., 1996. Treatment Wetlands. Lewis, Boca Raton, FL, 893 p.
Kazezyilmaz-Alhan, C.M., Medina Jr., M.A., Richardson, C.J., 2007. A wetland hydrology and water quality model incorporating surface water/groundwater interactions. Water Resources Research 43, W04434, doi:10.1029/2006WR005003.
Kushlan, J.A., 1990. Freshwater marshes. In: Meyers, R.L., Ewel, J.J. (Eds.), The ecosystems of Florida. University of Florida Press, Gainesville, FL, 324–363.
Lal, A.M.W., 1998. Weighted implicit finite-volume model for overland flow. Journal of Hydraulic Engineering 124 (9), 941–950.
Lal, A.M.W., 2000. Numerical errors in groundwater and overland flow models. Water Resources Research 36 (5), 1237–1247.

Lal, A.M.W., Van Zee, R., Belnap, M., 2005. Case study: model to simulate regional flow in south Florida. Journal of Hydraulic Engineering 131 (4), 247–258.
Langevin, C., Swain, E., Wolfert, M., 2005. Simulation of integrated surface-water/ground-water flow and salinity for a coastal wetland and adjacent estuary. Journal of Hydrology 314, 212–234.
Larsen, L.G., Harvey, J.W., Crimaldi, J.P., 2007. A delicate balance: ecohydrological feedbacks governing landscape morphology in a lotic peatland. Ecological Monographs 77 (4), 591–614.
Larsen, L.G., Harvey, J.W., Noe, G.B., Crimaldi, J.P., 2009. Predicting organic floc transport dynamics in shallow aquatic ecosystems: Insights from the field, the laboratory, and numerical modeling. Water Resources Research 45, W01411, doi:10.1029/2008WR007221.
Leonard, L., Croft, A., Childers, D., Mitchell-Bruker, S., Solo-Gabriele, H., Ross, M., 2006. Characteristics of surface-water flows in the ridge and slough landscape of Everglades National Park: implications for particulate transport. Hydrobiologia 569, 5–22.
Lightbody, A.F., Nepf, H.M., 2006. Prediction of velocity profiles and longitudinal dispersion in emergent salt marsh vegetation. Limnology and Oceanography 51 (1), 218–228.
Martinez, C.J., Wise, W.R., 2003. Hydraulic analysis of the Orlando easterly wetland. Journal of Environmental Engineering-ASCE 129, 553–560.
Min, J.H., Wise, W.R., 2009. Simulating short-circuiting flow in a constructed wetland: the implications of bathymetry and vegetation effects. Hydrological Processes 23, 830–841.
Min, J.H., Wise, W.R., 2010. Depth-averaged, spatially distributed flow dynamic and solute transport modeling of a large-scaled, subtropical constructed wetland. Hydrological processes, doi:10.1002/hyp.7686.
Nepf, H.M., 1999. Drag, turbulence, and diffusion in flow through emergent vegetation. Water Resources Research 35 (2), 479–489.
Noe, G.B., Childers, D.L., 2007. Phosphorus budgets in Everglades wetland ecosystems: the effects of hydrology and nutrient enrichment. Wetlands Ecology and Management 15, 189–205.
Noe, G.B., Harvey, J.W., Saiers, J.E., 2007. Characterization of suspended particles in Everglades wetlands. Limnology and Oceanography 52 (3), 1166–1178.
Palaseanu, M., Pearlstine, L., 2008. Estimation of water surface elevations for the Everglades, Florida. Computers and Geosciences 34, 815–826.
Paudel, R., Min, J.H., Jawitz, J.W., 2010. Management scenario evaluation for a large treatment wetland using a spatio-temporal phosphorus transport and cycling model. Ecological Engineering (In press).
Pearlstine, L., Higer, A., Palaseanu, M., Fujisaki, I., Mazzotti, F., 2007. Spatially continuous interpolation of water stage and water depth using the Everglades Depth Estimation Network (EDEN). University of Florida - IFAS Extension report CIR1521, 32 p.
Perry, W., 2004. Elements of South Florida’s Comprehensive Everglades Restoration Plan. Ecotoxicology 13, 185–193.

Ross, M.S., Mitchell-Bruker, S., Sah, J.P., Stothoff, S., Ruiz, P.L., Reed, D.L., Jayachandran, K., Coultas, C.L., 2006. Interaction of hydrology and nutrient limitation in the ridge and slough landscape of the southern Everglades. Hydrobiologia 569, 37–59.

Saiers, J.E., Harvey, J.W., Mylon, S.E., 2003. Surface water transport of suspended matter through wetland vegetation of the Florida Everglades. Geophysical Research Letters 30 (19), HLS 3-1 – HLS 3-5.

Schaffranek, R.W., Riscassi, A.L., Rybicki, N.B., Lombana, A.V., 2003. Fire effects on flow in vegetated wetlands of the Everglades. Greater Everglades Ecosystem Restoration conference, Palm Harbor, FL, USA, Apr. 13 – 18, 2003.

Science Coordination Team, 2003. The role of flow in the Everglades ridge and slough landscape. In: Aumen, N.G. (Ed.), South Florida Ecosystem Restoration Working Group. Available from: <http//sofia.usgs.gov/publications/paper/sct_flows>.

South Florida Water Management District, 1994. Natural System Model v4.2. SFWMD, West Palm Beach, FL. Available from: <https://my.sfwmd.gov/pls/portal/docs/PAGE/PG_GRP_SFWMD_HESM/PORTLET_NSM/PORTLET_SUBTAB_NSM_DOCUMENTS/TAB1354054/NSM_42.PDF>.

South Florida Water Management District, 2005a. Documentation of the South Florida Water Management Model v5.5. SFWMD, West Palm Beach, FL, 305 p.

South Florida Water Management District, 2005b. RSM user manual – HSE v1.0. SFWMD, West Palm Beach, FL, 286 p.

South Florida Water Management District, 2007. RSM technical reference manual – HSE theory manual v1.0. SFWMD, West Palm Beach, FL, 44 p.

Sutron Corp., 2004. STA-6 2-D hydraulic modeling – task 2.3.1 final report prepared for South Florida Water Management District, October 27, 2004.

Swain, E.D., 2005. A model for simulation of surface-water integrated flow and transport in two dimensions: user's guide for application to coastal wetlands. U.S. Geological Survey Open-File Report 2005-1033, 88 p.

Townsend, P.A., 2001. Relationships between vegetation patterns and hydroperiod on the Roanoke River floodplain, North Carolina. Plant Ecology 156, 43–58.

Wu, Y., Wang, N., Rutchey, K., 2006. An analysis of spatial complexity of ridge and slough patterns in the Everglades ecosystem. Ecological Complexity 3, 183–192.

Table 1. Wetland flow frictional equations tested in this study.

		Model parameters			R^2		Bias		RMSE		N-S	
	R/S[*]	*A*	*b*	*c*	*v*	*h*[**]	*v* (cm/s)	*h*[**] (m)	*v* (cm/s)	*h*[**] (m)	*v*	*h*[**]
Kadlec and Knight (1996)[§]	R	1.0×10^{7} $m^{-1}d^{-1}$	3.0	1.0	0.78	0.98	-0.42	0.030	0.508	0.039	-1.22	0.96
	S	5.0×10^{7} $m^{-1}d^{-1}$	3.0	1.0	0.95		-0.28		0.403		0.40	
Bolster and Saiers (2002)[§§]	R	5.1×10^{6} $m^{0.46}d^{-1}$	1.54	1.0	0.74	0.99	-0.41	0.031	0.505	0.039	-1.21	0.96
	S	5.1×10^{6} $m^{0.46}d^{-1}$	1.54	1.0	0.73		-0.44		0.650		-0.55	
Kadlec-type	R	1.25×10^{8} $m^{-1}d^{-1}$[†]	3.0	1.0	0.76	0.98	-0.11	0.032	0.209	0.041	0.62	0.96
	S	1.04×10^{8} $m^{-1}d^{-1}$[†]	3.0	1.0	0.95		0.02		0.111		0.95	
Modified Manning (*d*-dependent *n*)[††]	R	3.1×10^{4} ~ 3.5×10^{5} $m^{0.33}d^{-1}$[†]	1.67	0.5	0.86	0.98	-0.05	0.030	0.139	0.039	0.83	0.96
	S	4.4×10^{4} ~ 4.6×10^{5} $m^{0.33}d^{-1}$[†]	1.67	0.5	0.90		0.07		0.143		0.93	
Manning[¶]	R	6.9×10^{5} $m^{0.33}d^{-1}$[†]	1.67	0.5	0.62	0.98	0.05	0.030	0.171	0.038	0.75	0.96
	S	7.8×10^{5} $m^{0.33}d^{-1}$[†]	1.67	0.5	0.51		0.10		0.245		0.78	

[*]R = Ridge / S = Slough, [**]Calibrated to *h* measured at 3A-S (this study), [§]Recommended values (R: densely / S: sparsely vegetated), [§§]Calibrated to Shark River Slough *h*, [†]Calibrated to *v* measured at J-1 (this study), [††]*A* = 0.19 (R) / 0.17 (S), [¶]*n* = 0.13 (R) / 0.11 $s/m^{1/3}$ (S).

Table 2. Summary of transport modeling setup through imaginary mass injection and the simulated hydrodynamic condition.

	Flow regime	Current		Restored	
		Dry	Wet	Dry	Wet
RSM + TaRSE model setup	Simulation period	3/1/02-3/31/02	8/1/02-8/31/02	3/1/02-3/31/02	8/1/02-8/31/02
	Simulation time step	10 minute			
	Mass injected	30 kg			
	Rainfall and ET	Excluded			
	Boundary condition	Measured WL (upper/lower boundary)		Measured WL + 0.20 m	
	α_L	20 m**			
	α_T	2 m**			
Flow dynamic condition*	Water depth	0.29 m	0.62 m	0.49 m	0.82 m
	Flow velocity	0.4 cm/s	0.8 cm/s	0.8 cm/s	1.2 cm/s

* Average hydrodynamic condition at tracer injection slough grid cell (asterisk in Fig. 3).
** Average dispersion coefficient values calculated with these dispersivities were within the range suggested by Ho et al. (2009).

Table 3. Comparison between measured and simulated hydraulic heads (*h* and *d*).

		N	Mean	SD	Max.	Min.	Note
h (m)	Measured	1096	3.27	0.19	3.72	2.80	3A-S (Slough: USGS, EDEN)
	Simulated	1096	3.30	0.19	3.75	2.92	
d (m)	Measured	67	0.43	0.20	0.92	0.14	CA311 (Slough: SFWMD, DBHYDRO)
	Simulated	1096	0.41	0.19	0.87	0.04	

Table 4. Sensitivity of modeled *v* in the ridges and sloughs to change in hydraulic resistance coefficient, *A* (±30%).

	Model calibration			30% increase in *A*			30% decrease in *A*		
	A	Avg. *v* ± 1 SD (cm/s)	RMSE (cm/s)	*A*	RMSE (cm/s)	$S_{v,A}$*	*A*	RMSE (cm/s)	$S_{v,A}$*
Ridge	0.19	0.47 ± 0.40	0.139	0.25	0.198	-0.73	0.13	0.272	-1.34
Slough	0.17	0.66 ± 0.49	0.143	0.22	0.201	-0.74	0.12	0.325	-1.30

* Sensitivity coefficients defined as the ratio of the change of 3 year-averaged simulated *v* to the change of hydraulic resistance coefficient, *A* for ±30% change in the coefficient.

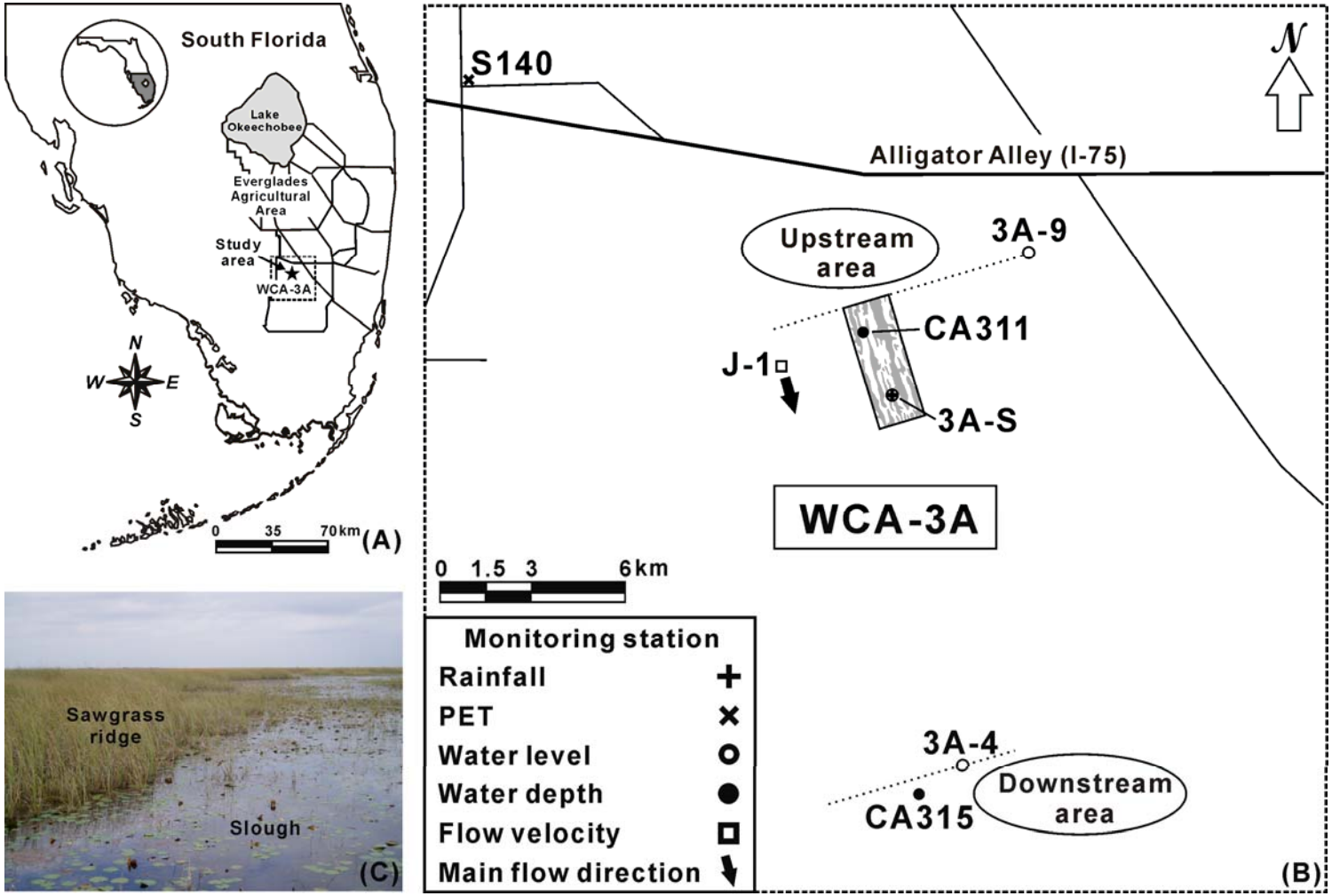

Figure 1. Location maps of model domain and hydrometeorologic data monitoring stations: (A) Regional map of study area in Water Conservation Area 3A, (B) Enlarged view of study area (dotted rectangle in panel A) showing the location of model domain and hydrometeorologic data monitoring stations used for model development and calibration. The station numbers are from the SFWMD online database DBHYDRO, except station J-1, from Jorczak (2006), and (C) Photograph showing the typical sawgrass-dominant ridge and open slough landscape in study area

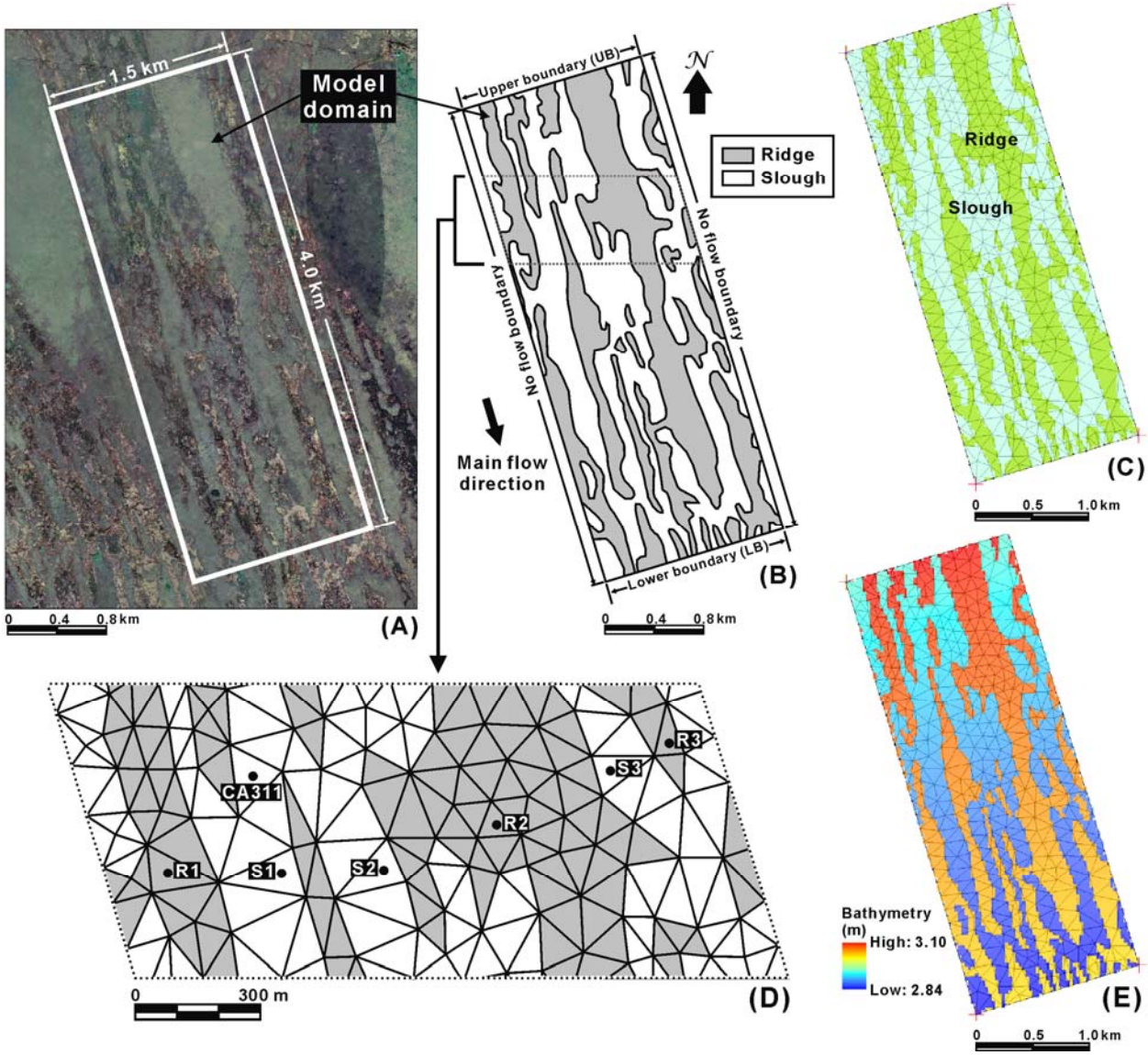

Figure 2. Model domain – the bimodal landscape and the spatially distributed key model input data: (A) The selected 1.5 by 4.0 km rectangular model domain, parallel to the elongated axis of the ridges, (B) The model domain classified into two dominant aquatic habitats (ridge and slough) according to the bimodal landscape pattern delineated by Cowardin et al. (1979) and the assigned model boundary conditions (note that no flow boundary was assumed for both directions perpendicular to the main flow direction), (C) 2-D, irregular triangular grid mesh overlapped onto the bimodal landscape pattern, (D) Specific grid cell location of simulation output points for *d* and *v*, and (E) Model bathymetry prediction map interpolated using spline.

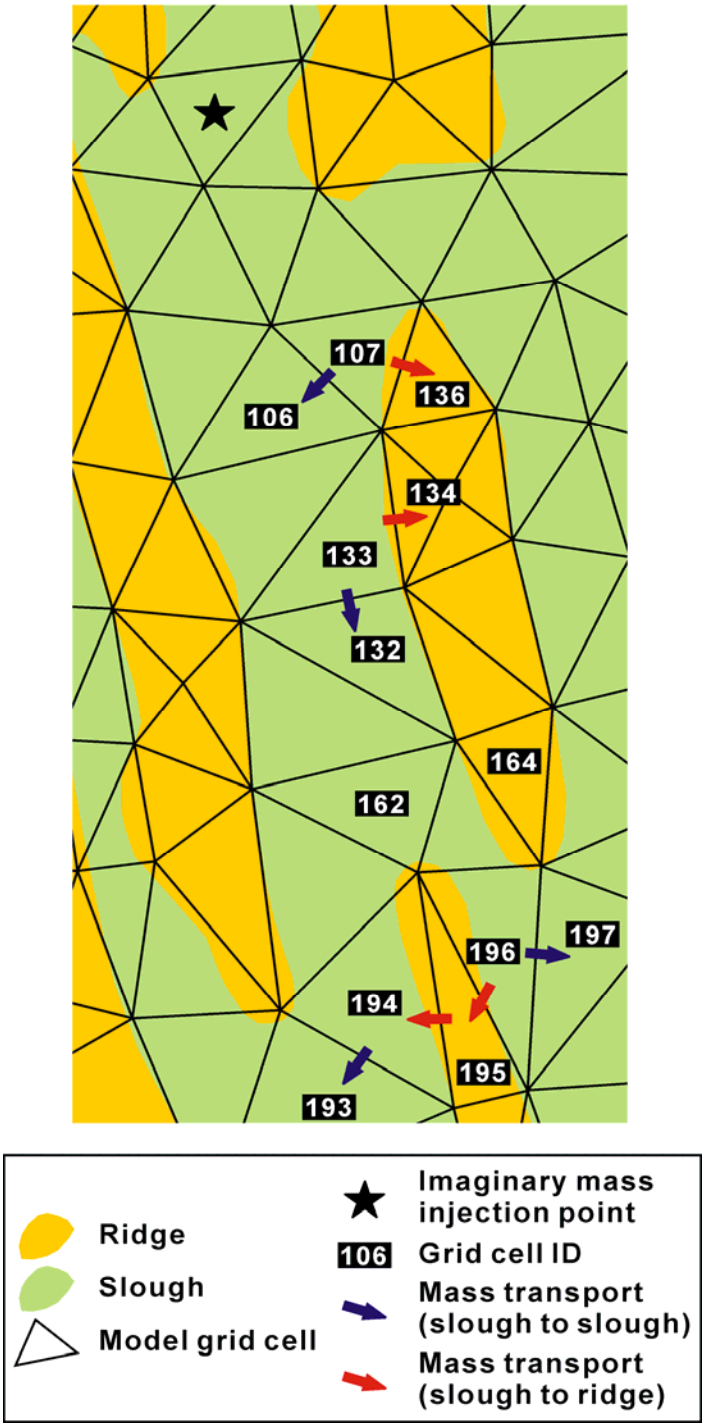

Figure 3. Location of simulated mass injection and the simulation output points.

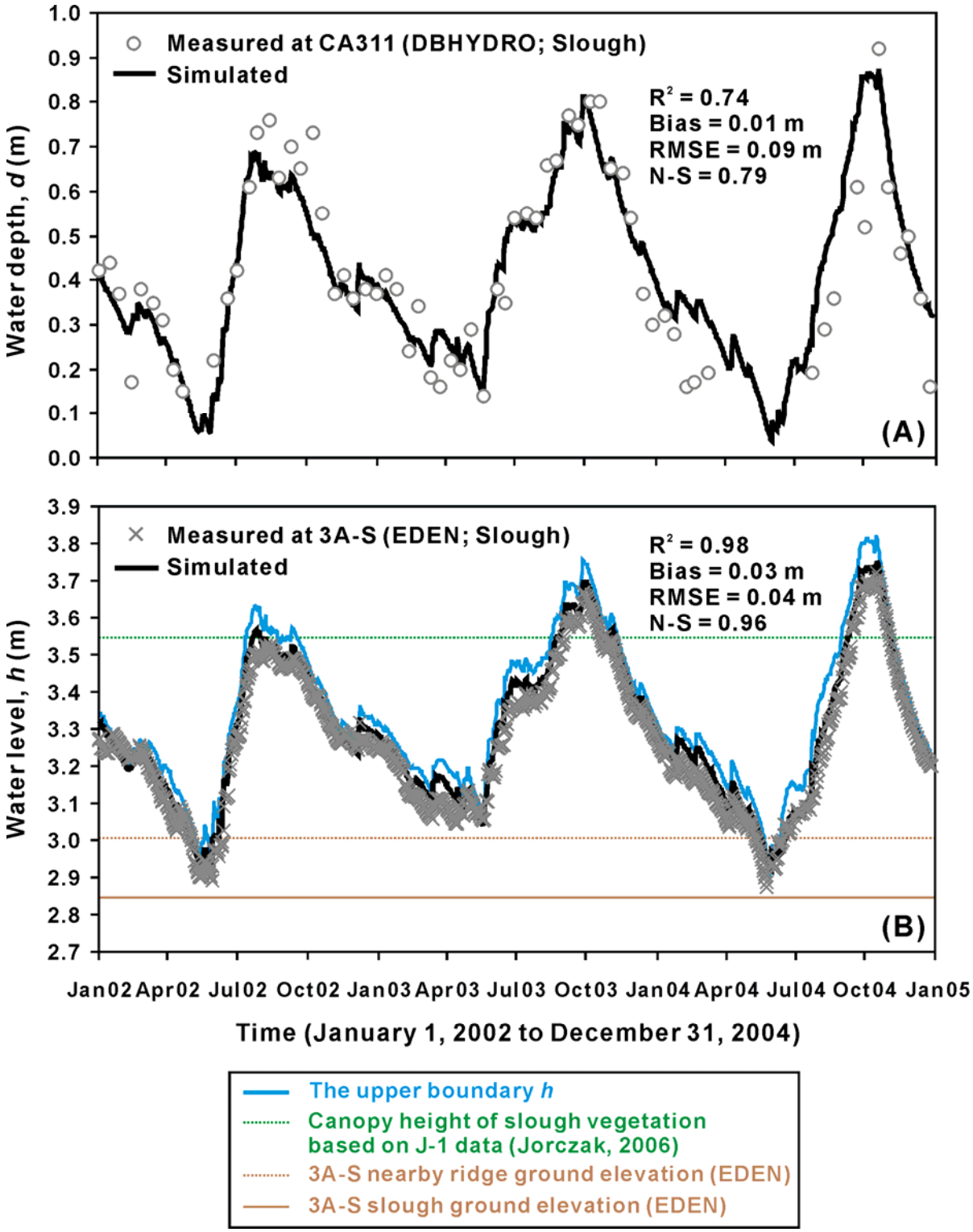

Figure 4. Model fit of time series hydraulic head measured at two interior points of model domain: (A) *d* at CA311 and (B) *h* at 3A-S. The canopy height of ridge vegetation (sawgrass: about 2 m above the ridge ground elevation) is not marked (out of range of y axis).

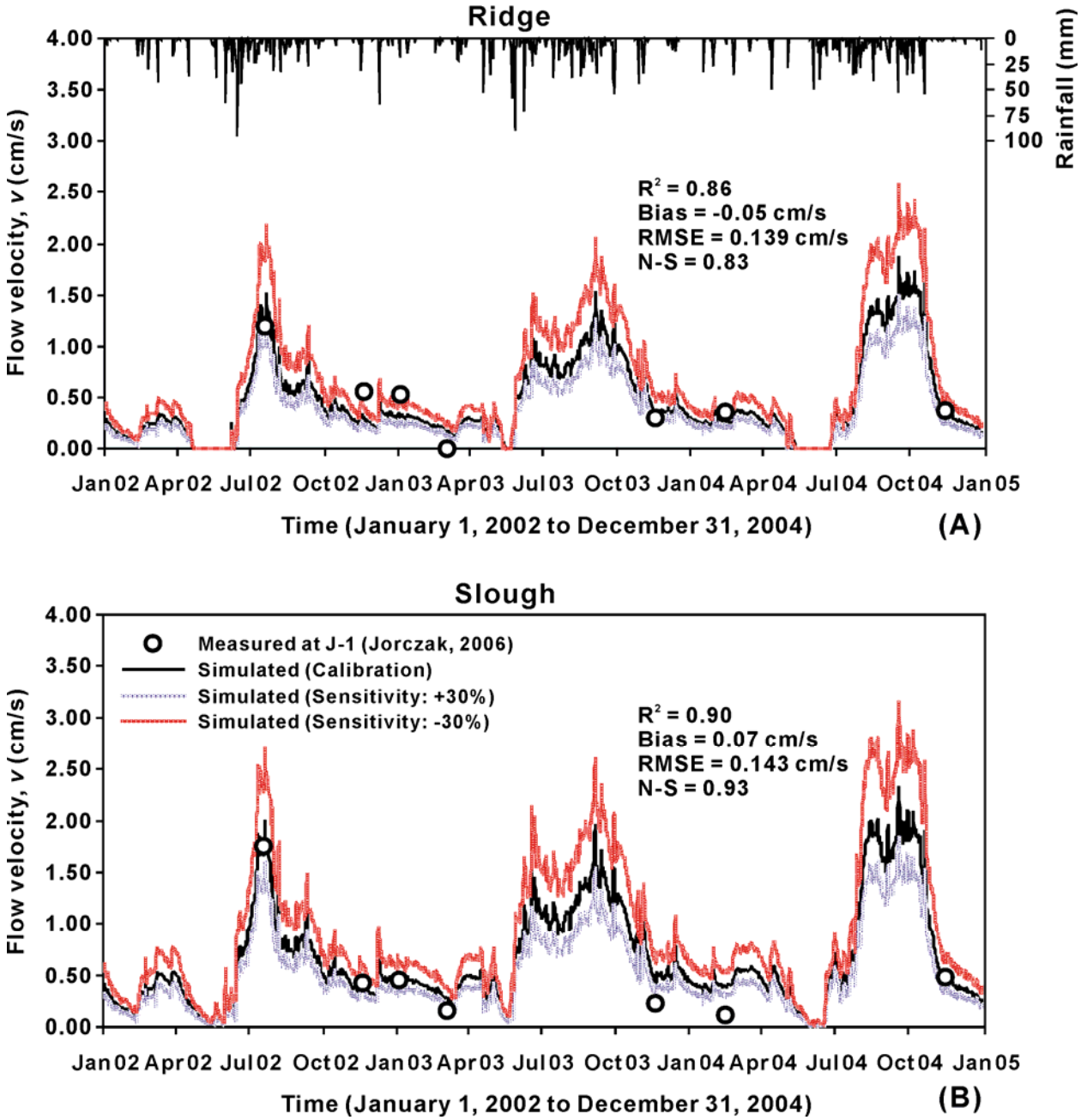

Figure 5. Model fit of *v* measured at J-1 by Jorczak (2006) and sensitivities of model-calculated flow velocities to change in hydraulic resistance coefficient, *A* (±30%): (A) Ridge and (B) Slough. For model calibration, average of *v* profiles simulated at R1-3 and S1-3 was used, respectively.

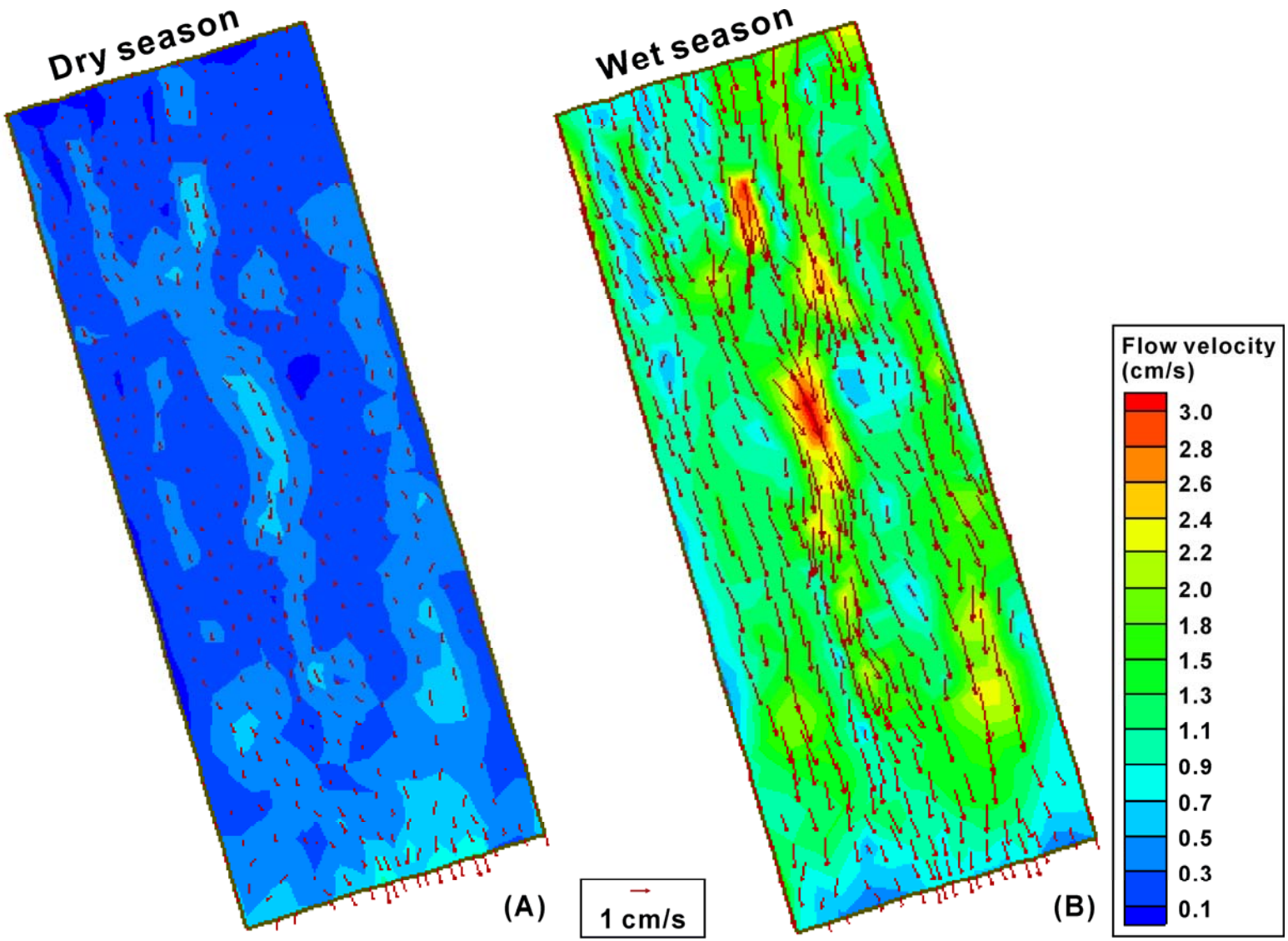

Figure 6. Snapshots of computed *v* in the model domain: (A) Dry season (April 20, 2004) and (B) Wet season (August 24, 2004).

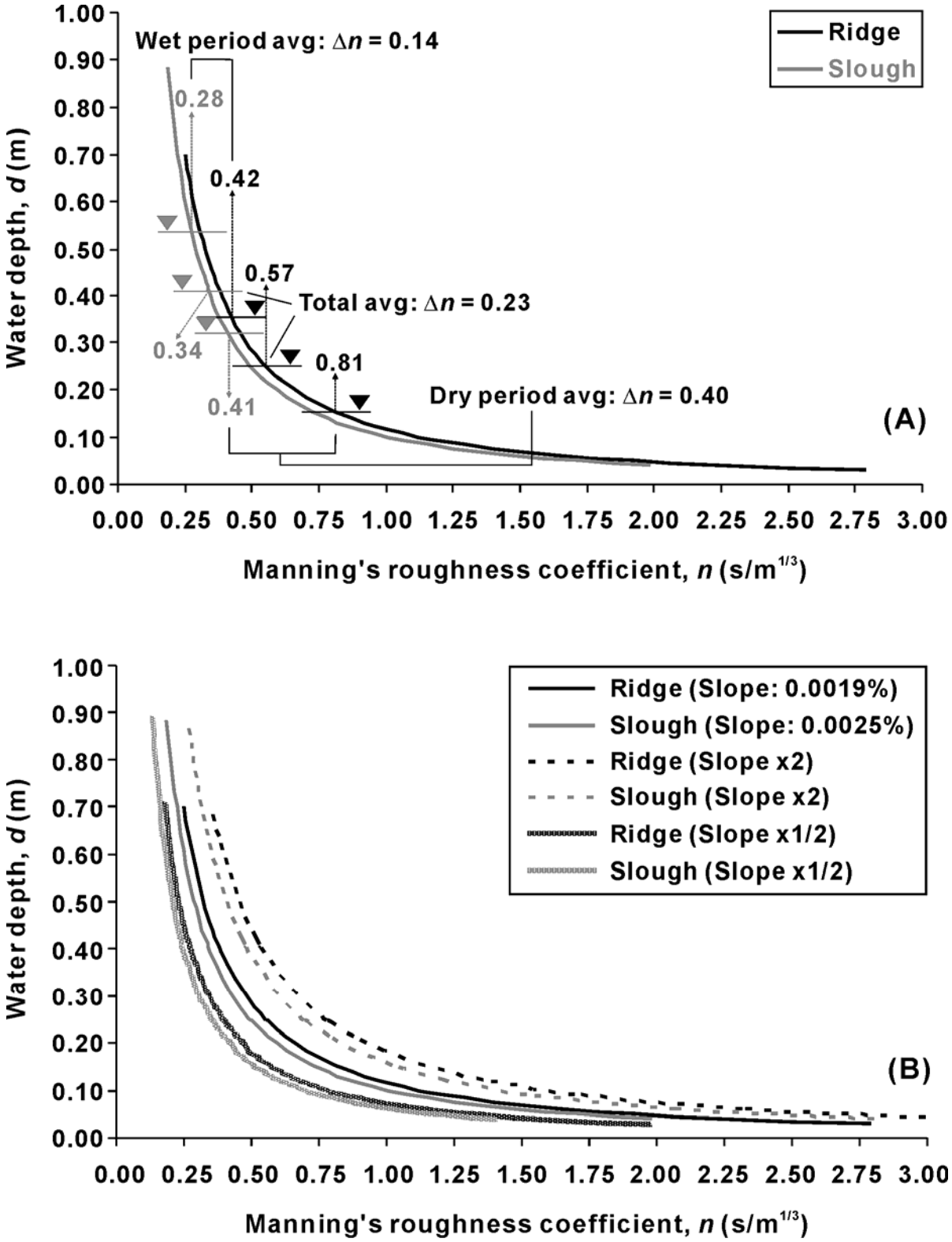

Figure 7. Relationship between Manning's roughness coefficient and *d* in the ridges and sloughs: (A) Model calibration result and (B) The impact of changes in topographic slopes (×2 and ×0.5).

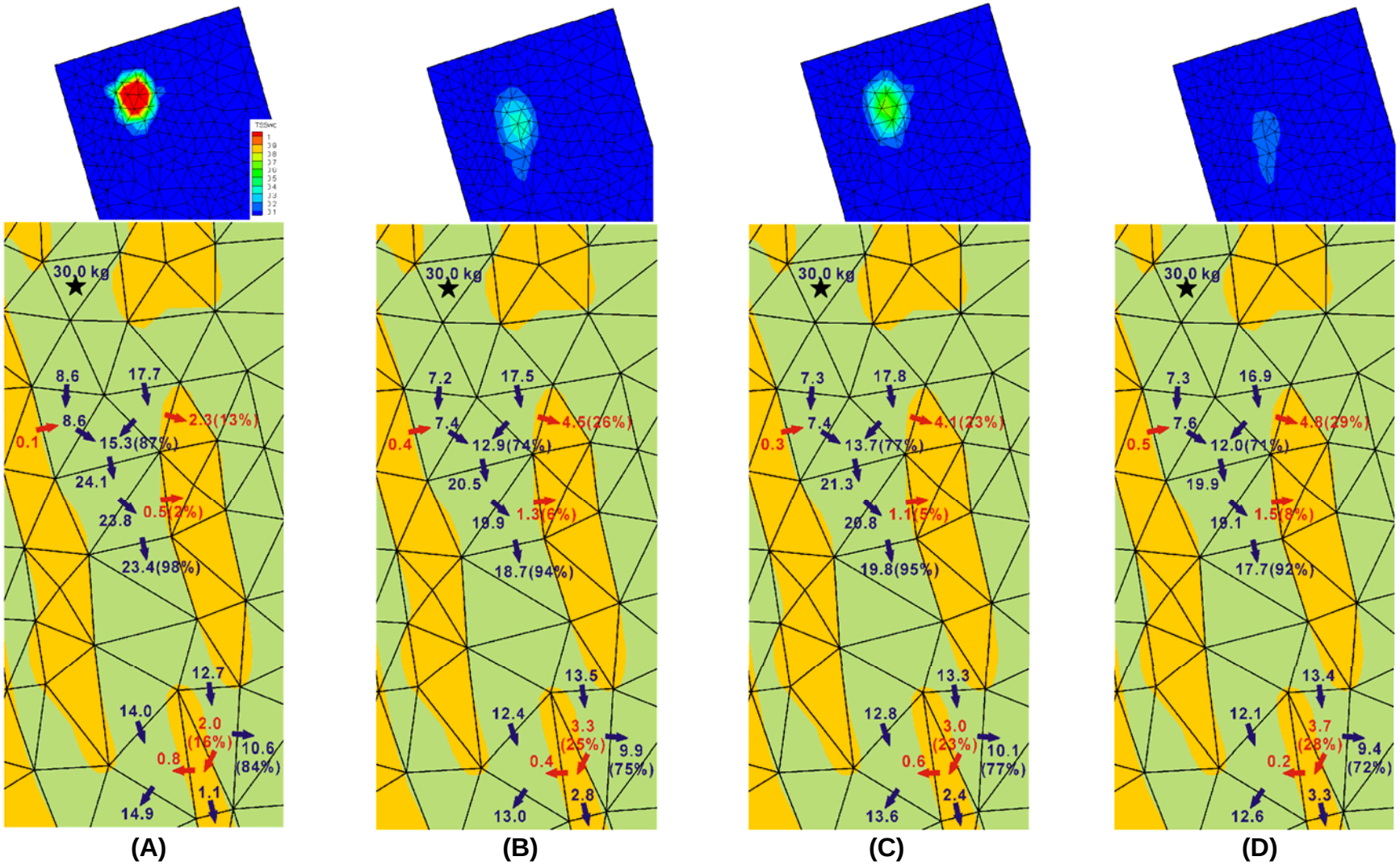

Figure 8. Snapshots of plume (tracer concentration in water column) after 1 day from the mass injection time and grid cell-based total mass transfer during the simulation period: (a) current dry, (b) current wet, (c) restored dry, and (d) restored wet flow regime.

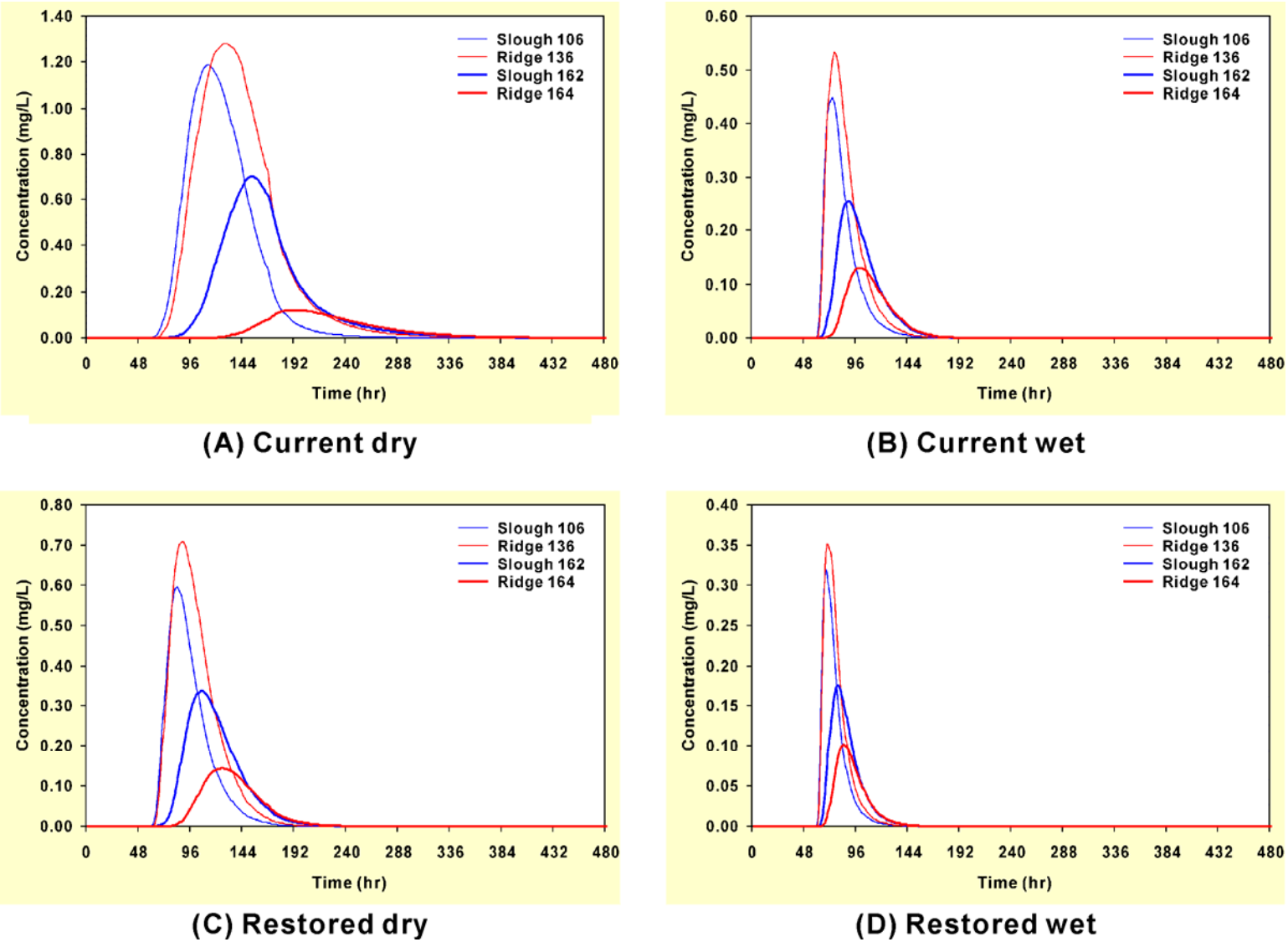

Figure 9. BTCs at downstream ridge and slough grid cells (Cell ID 106/136: 250 m and Cell ID 162/164: 580 m apart from the injection point).

Appendix A. Two-dimensional GMS mesh data file of the model domain

```
MESH2D
E3T   1   2   3   1   1
E3T   2   1   3   4   1
E3T   3   1   4   5   1
E3T   4   3   2   6   1
E3T   5   3   6   7   1
E3T   6   3   7   8   1
E3T   7   9   3   8   1
E3T   8   9   4   3   1
E3T   9  10   4   9   1
E3T  10   5   4  10   1
E3T  11   5  10  11   1
E3T  12  11  12   5   1
E3T  13   7   6  13   1
E3T  14  13  14   7   1
E3T  15   7  14   8   1
E3T  16   8  14  15   1
E3T  17   8  15   9   1
E3T  18  15  16   9   1
E3T  19   9  16  17   1
E3T  20  18   9  17   1
E3T  21   9  18  10   1
E3T  22  10  18  11   1
E3T  23  18  19  11   1
E3T  24  20  11  19   1
E3T  25  21  11  20   1
E3T  26  12  11  21   1
E3T  27  13  22  23   1
E3T  28  23  14  13   1
E3T  29  23  24  14   1
E3T  30  14  24  25   1
E3T  31  15  14  25   1
E3T  32  25  16  15   1
E3T  33  26  16  25   1
E3T  34  16  26  27   1
E3T  35  17  16  27   1
E3T  36  17  27  28   1
E3T  37  29  17  28   1
E3T  38  17  29  18   1
E3T  39  19  18  29   1
E3T  40  29  30  19   1
E3T  41  31  19  30   1
E3T  42  20  19  31   1
E3T  43  31  32  20   1
E3T  44  32  21  20   1
E3T  45  21  32  33   1
E3T  46  22  34  24   1
E3T  47  23  22  24   1
E3T  48  34  35  24   1
E3T  49  24  35  36   1
E3T  50  24  36  37   1
E3T  51  24  37  25   1
E3T  52  26  25  37   1
E3T  53  37  38  26   1
E3T  54  26  38  39   1
E3T  55  39  27  26   1
E3T  56  39  40  27   1
E3T  57  28  27  40   1
E3T  58  28  40  41   1
E3T  59  28  41  42   1
E3T  60  28  42  43   1
E3T  61  28  43  30   1
E3T  62  28  30  29   1
E3T  63  30  43  44   1
E3T  64  31  30  44   1
E3T  65  32  31  44   1
E3T  66  44  45  32   1
E3T  67  32  45  46   1
E3T  68  46  33  32   1
E3T  69  46  47  33   1
E3T  70  35  34  48   1
E3T  71  49  35  48   1
E3T  72  36  35  49   1
E3T  73  50  36  49   1
E3T  74  36  50  38   1
E3T  75  37  36  38   1
E3T  76  51  38  50   1
E3T  77  38  51  52   1
E3T  78  38  52  39   1
E3T  79  41  39  52   1
E3T  80  40  39  41   1
E3T  81  53  41  52   1
E3T  82  53  54  41   1
E3T  83  41  54  42   1
E3T  84  42  54  55   1
E3T  85  42  55  56   1
E3T  86  43  42  56   1
E3T  87  56  45  43   1
E3T  88  43  45  44   1
E3T  89  56  57  45   1
E3T  90  46  45  57   1
E3T  91  58  46  57   1
E3T  92  59  46  58   1
E3T  93  46  59  47   1
E3T  94  48  60  61   1
E3T  95  61  62  48   1
E3T  96  62  49  48   1
E3T  97  49  62  63   1
E3T  98  50  49  63   1
E3T  99  51  50  63   1
E3T 100  63  64  51   1
E3T 101  65  51  64   1
E3T 102  51  65  52   1
E3T 103  52  65  53   1
E3T 104  65  66  53   1
E3T 105  66  67  53   1
E3T 106  67  54  53   1
E3T 107  54  67  68   1
E3T 108  68  55  54   1
E3T 109  55  68  69   1
E3T 110  69  70  55   1
E3T 111  56  55  70   1
E3T 112  57  56  70   1
E3T 113  70  71  57   1
E3T 114  57  71  72   1
E3T 115  58  57  72   1
E3T 116  72  73  58   1
E3T 117  58  73  59   1
E3T 118  59  73  74   1
E3T 119  75  76  60   1
E3T 120  61  60  76   1
E3T 121  76  62  61   1
E3T 122  62  76  63   1
E3T 123  77  63  76   1
E3T 124  63  77  64   1
E3T 125  77  78  64   1
E3T 126  64  78  79   1
E3T 127  79  65  64   1
E3T 128  80  65  79   1
E3T 129  80  66  65   1
E3T 130  66  80  81   1
E3T 131  66  81  82   1
E3T 132  83  66  82   1
E3T 133  67  66  83   1
```

E3T	134	83	84	67	1
E3T	135	67	84	85	1
E3T	136	85	68	67	1
E3T	137	68	85	86	1
E3T	138	69	68	86	1
E3T	139	86	87	69	1
E3T	140	88	69	87	1
E3T	141	88	71	69	1
E3T	142	70	69	71	1
E3T	143	88	89	71	1
E3T	144	72	71	89	1
E3T	145	72	89	90	1
E3T	146	73	72	90	1
E3T	147	91	73	90	1
E3T	148	74	73	91	1
E3T	149	75	92	93	1
E3T	150	75	93	94	1
E3T	151	94	76	75	1
E3T	152	77	76	94	1
E3T	153	94	95	77	1
E3T	154	77	95	78	1
E3T	155	95	96	78	1
E3T	156	96	97	78	1
E3T	157	78	97	79	1
E3T	158	81	79	97	1
E3T	159	81	80	79	1
E3T	160	81	97	98	1
E3T	161	99	81	98	1
E3T	162	81	99	82	1
E3T	163	82	99	100	1
E3T	164	82	100	101	1
E3T	165	83	82	101	1
E3T	166	102	83	101	1
E3T	167	84	83	102	1
E3T	168	85	84	102	1
E3T	169	102	103	85	1
E3T	170	85	103	86	1
E3T	171	104	86	103	1
E3T	172	87	86	104	1
E3T	173	104	105	87	1
E3T	174	106	87	105	1
E3T	175	106	107	87	1
E3T	176	88	87	107	1
E3T	177	88	107	108	1
E3T	178	89	88	108	1
E3T	179	109	89	108	1
E3T	180	89	109	90	1
E3T	181	110	90	109	1
E3T	182	91	90	110	1
E3T	183	111	91	110	1
E3T	184	113	92	112	1
E3T	185	113	114	92	1
E3T	186	93	92	114	1
E3T	187	114	94	93	1
E3T	188	114	95	94	1
E3T	189	96	95	114	1
E3T	190	114	115	96	1
E3T	191	115	98	96	1
E3T	192	98	97	96	1
E3T	193	98	115	116	1
E3T	194	116	99	98	1
E3T	195	99	116	117	1
E3T	196	117	100	99	1
E3T	197	117	118	100	1
E3T	198	100	118	119	1
E3T	199	119	101	100	1
E3T	200	120	101	119	1
E3T	201	120	121	101	1
E3T	202	121	102	101	1
E3T	203	103	102	121	1
E3T	204	121	122	103	1
E3T	205	122	104	103	1
E3T	206	122	105	104	1
E3T	207	123	105	122	1
E3T	208	105	123	124	1
E3T	209	106	105	124	1
E3T	210	125	106	124	1
E3T	211	126	106	125	1
E3T	212	106	126	107	1
E3T	213	127	107	126	1
E3T	214	128	107	127	1
E3T	215	128	108	107	1
E3T	216	128	109	108	1
E3T	217	129	109	128	1
E3T	218	110	109	129	1
E3T	219	110	129	130	1
E3T	220	110	130	111	1
E3T	221	132	112	131	1
E3T	222	132	113	112	1
E3T	223	114	113	132	1
E3T	224	114	132	115	1
E3T	225	115	132	133	1
E3T	226	134	115	133	1
E3T	227	135	115	134	1
E3T	228	116	115	135	1
E3T	229	117	116	135	1
E3T	230	117	135	136	1
E3T	231	137	117	136	1
E3T	232	117	137	118	1
E3T	233	138	118	137	1
E3T	234	118	138	119	1
E3T	235	119	138	139	1
E3T	236	120	119	139	1
E3T	237	139	140	120	1
E3T	238	120	140	121	1
E3T	239	121	140	122	1
E3T	240	140	123	122	1
E3T	241	123	140	141	1
E3T	242	123	141	142	1
E3T	243	124	123	142	1
E3T	244	125	124	142	1
E3T	245	143	125	142	1
E3T	246	125	143	144	1
E3T	247	144	145	125	1
E3T	248	126	125	145	1
E3T	249	146	126	145	1
E3T	250	146	127	126	1
E3T	251	127	146	147	1
E3T	252	128	127	147	1
E3T	253	148	128	147	1
E3T	254	128	148	129	1
E3T	255	148	149	129	1
E3T	256	129	149	150	1
E3T	257	130	129	150	1
E3T	258	131	151	152	1
E3T	259	131	152	132	1
E3T	260	132	152	133	1
E3T	261	133	152	153	1
E3T	262	153	134	133	1
E3T	263	153	154	134	1
E3T	264	154	155	134	1
E3T	265	135	134	155	1
E3T	266	156	135	155	1
E3T	267	135	156	136	1
E3T	268	136	156	157	1
E3T	269	157	158	136	1
E3T	270	158	159	136	1
E3T	271	159	137	136	1
E3T	272	159	160	137	1
E3T	273	161	137	160	1

E3T	274	137	161	138	1
E3T	275	161	162	138	1
E3T	276	162	163	138	1
E3T	277	138	163	164	1
E3T	278	139	138	164	1
E3T	279	139	164	141	1
E3T	280	141	140	139	1
E3T	281	141	164	165	1
E3T	282	142	141	165	1
E3T	283	165	143	142	1
E3T	284	165	166	143	1
E3T	285	143	166	167	1
E3T	286	143	167	144	1
E3T	287	168	144	167	1
E3T	288	168	169	144	1
E3T	289	144	169	145	1
E3T	290	146	145	169	1
E3T	291	146	169	170	1
E3T	292	170	147	146	1
E3T	293	171	147	170	1
E3T	294	171	172	147	1
E3T	295	172	148	147	1
E3T	296	149	148	172	1
E3T	297	173	149	172	1
E3T	298	149	173	150	1
E3T	299	174	150	173	1
E3T	300	151	175	176	1
E3T	301	176	152	151	1
E3T	302	153	152	176	1
E3T	303	177	153	176	1
E3T	304	154	153	177	1
E3T	305	177	178	154	1
E3T	306	178	179	154	1
E3T	307	179	155	154	1
E3T	308	179	180	155	1
E3T	309	155	180	156	1
E3T	310	157	156	180	1
E3T	311	181	157	180	1
E3T	312	157	181	182	1
E3T	313	158	157	182	1
E3T	314	182	183	158	1
E3T	315	158	183	184	1
E3T	316	184	159	158	1
E3T	317	159	184	160	1
E3T	318	184	185	160	1
E3T	319	161	160	185	1
E3T	320	161	185	186	1
E3T	321	162	161	186	1
E3T	322	186	187	162	1
E3T	323	187	163	162	1
E3T	324	163	187	188	1
E3T	325	188	189	163	1
E3T	326	189	164	163	1
E3T	327	189	165	164	1
E3T	328	166	165	189	1
E3T	329	189	190	166	1
E3T	330	190	191	166	1
E3T	331	191	167	166	1
E3T	332	191	192	167	1
E3T	333	167	192	168	1
E3T	334	193	168	192	1
E3T	335	194	168	193	1
E3T	336	195	168	194	1
E3T	337	169	168	195	1
E3T	338	169	195	170	1
E3T	339	170	195	196	1
E3T	340	170	196	197	1
E3T	341	170	197	171	1
E3T	342	198	171	197	1
E3T	343	171	198	199	1
E3T	344	199	172	171	1
E3T	345	199	173	172	1
E3T	346	174	173	199	1
E3T	347	199	200	174	1
E3T	348	175	201	202	1
E3T	349	202	203	175	1
E3T	350	176	175	203	1
E3T	351	177	176	203	1
E3T	352	203	178	177	1
E3T	353	178	203	204	1
E3T	354	178	204	179	1
E3T	355	205	179	204	1
E3T	356	206	179	205	1
E3T	357	180	179	206	1
E3T	358	180	206	181	1
E3T	359	181	206	207	1
E3T	360	207	208	181	1
E3T	361	182	181	208	1
E3T	362	182	208	209	1
E3T	363	183	182	209	1
E3T	364	183	209	210	1
E3T	365	184	183	210	1
E3T	366	184	210	185	1
E3T	367	210	211	185	1
E3T	368	211	186	185	1
E3T	369	186	211	212	1
E3T	370	186	212	187	1
E3T	371	213	187	212	1
E3T	372	188	187	213	1
E3T	373	213	214	188	1
E3T	374	188	214	190	1
E3T	375	188	190	189	1
E3T	376	190	214	215	1
E3T	377	190	215	216	1
E3T	378	216	191	190	1
E3T	379	191	216	217	1
E3T	380	192	191	217	1
E3T	381	193	192	217	1
E3T	382	218	193	217	1
E3T	383	218	219	193	1
E3T	384	219	220	193	1
E3T	385	193	220	194	1
E3T	386	194	220	221	1
E3T	387	194	221	195	1
E3T	388	195	221	196	1
E3T	389	198	222	200	1
E3T	390	200	199	198	1
E3T	391	223	224	201	1
E3T	392	201	224	202	1
E3T	393	202	224	204	1
E3T	394	204	203	202	1
E3T	395	224	205	204	1
E3T	396	205	224	225	1
E3T	397	205	225	226	1
E3T	398	205	226	206	1
E3T	399	207	206	226	1
E3T	400	207	226	227	1
E3T	401	207	227	228	1
E3T	402	208	207	228	1
E3T	403	208	228	229	1
E3T	404	229	209	208	1
E3T	405	229	230	209	1
E3T	406	210	209	230	1
E3T	407	231	210	230	1
E3T	408	231	211	210	1
E3T	409	211	231	232	1
E3T	410	212	211	232	1
E3T	411	212	232	233	1
E3T	412	212	233	234	1
E3T	413	212	234	213	1

E3T	414	213	234	214	1
E3T	415	235	214	234	1
E3T	416	214	235	215	1
E3T	417	215	235	236	1
E3T	418	215	236	218	1
E3T	419	218	216	215	1
E3T	420	218	217	216	1
E3T	421	218	236	219	1
E3T	422	237	219	236	1
E3T	423	238	219	237	1
E3T	424	239	219	238	1
E3T	425	219	239	220	1
E3T	426	223	240	241	1
E3T	427	241	224	223	1
E3T	428	225	224	241	1
E3T	429	242	225	241	1
E3T	430	225	242	243	1
E3T	431	225	243	226	1
E3T	432	243	244	226	1
E3T	433	245	226	244	1
E3T	434	227	226	245	1
E3T	435	245	246	227	1
E3T	436	247	227	246	1
E3T	437	227	247	248	1
E3T	438	227	248	228	1
E3T	439	228	248	249	1
E3T	440	249	229	228	1
E3T	441	250	229	249	1
E3T	442	229	250	230	1
E3T	443	250	251	230	1
E3T	444	230	251	231	1
E3T	445	231	251	252	1
E3T	446	252	253	231	1
E3T	447	253	232	231	1
E3T	448	253	233	232	1
E3T	449	254	233	253	1
E3T	450	234	233	254	1
E3T	451	234	254	235	1
E3T	452	255	235	254	1
E3T	453	236	235	255	1
E3T	454	255	256	236	1
E3T	455	256	237	236	1
E3T	456	257	237	256	1
E3T	457	238	237	257	1
E3T	458	259	240	258	1
E3T	459	259	242	240	1
E3T	460	242	241	240	1
E3T	461	242	259	243	1
E3T	462	259	260	243	1
E3T	463	243	260	244	1
E3T	464	244	260	261	1
E3T	465	261	262	244	1
E3T	466	262	245	244	1
E3T	467	263	245	262	1
E3T	468	246	245	263	1
E3T	469	263	264	246	1
E3T	470	247	246	264	1
E3T	471	265	247	264	1
E3T	472	266	247	265	1
E3T	473	266	267	247	1
E3T	474	247	267	248	1
E3T	475	249	248	267	1
E3T	476	268	249	267	1
E3T	477	249	268	250	1
E3T	478	250	268	269	1
E3T	479	270	250	269	1
E3T	480	250	270	251	1
E3T	481	251	270	252	1
E3T	482	252	270	271	1
E3T	483	252	271	272	1
E3T	484	252	272	253	1
E3T	485	253	272	273	1
E3T	486	254	253	273	1
E3T	487	254	273	255	1
E3T	488	273	274	255	1
E3T	489	274	256	255	1
E3T	490	275	256	274	1
E3T	491	256	275	257	1
E3T	492	257	275	276	1
E3T	493	278	258	277	1
E3T	494	278	259	258	1
E3T	495	260	259	278	1
E3T	496	278	279	260	1
E3T	497	280	260	279	1
E3T	498	261	260	280	1
E3T	499	280	281	261	1
E3T	500	282	261	281	1
E3T	501	262	261	282	1
E3T	502	282	283	262	1
E3T	503	262	283	263	1
E3T	504	263	283	264	1
E3T	505	283	284	264	1
E3T	506	285	264	284	1
E3T	507	264	285	265	1
E3T	508	265	285	286	1
E3T	509	265	286	266	1
E3T	510	287	266	286	1
E3T	511	266	287	267	1
E3T	512	287	288	267	1
E3T	513	288	268	267	1
E3T	514	269	268	288	1
E3T	515	288	289	269	1
E3T	516	289	290	269	1
E3T	517	290	270	269	1
E3T	518	270	290	271	1
E3T	519	271	290	291	1
E3T	520	272	271	291	1
E3T	521	292	272	291	1
E3T	522	273	272	292	1
E3T	523	274	273	292	1
E3T	524	274	292	293	1
E3T	525	293	275	274	1
E3T	526	293	294	275	1
E3T	527	295	275	294	1
E3T	528	295	276	275	1
E3T	529	277	296	279	1
E3T	530	279	278	277	1
E3T	531	296	297	279	1
E3T	532	279	297	280	1
E3T	533	280	297	298	1
E3T	534	281	280	298	1
E3T	535	281	298	299	1
E3T	536	282	281	299	1
E3T	537	299	300	282	1
E3T	538	300	283	282	1
E3T	539	284	283	300	1
E3T	540	284	300	301	1
E3T	541	284	301	285	1
E3T	542	302	285	301	1
E3T	543	285	302	286	1
E3T	544	286	302	303	1
E3T	545	303	304	286	1
E3T	546	287	286	304	1
E3T	547	304	305	287	1
E3T	548	287	305	288	1
E3T	549	288	305	306	1
E3T	550	289	288	306	1
E3T	551	289	306	307	1
E3T	552	289	307	308	1
E3T	553	289	308	309	1

E3T	554	309	290	289	1
E3T	555	290	309	310	1
E3T	556	291	290	310	1
E3T	557	311	291	310	1
E3T	558	291	311	292	1
E3T	559	292	311	293	1
E3T	560	312	293	311	1
E3T	561	312	294	293	1
E3T	562	312	313	294	1
E3T	563	294	313	314	1
E3T	564	295	294	314	1
E3T	565	297	296	315	1
E3T	566	316	297	315	1
E3T	567	298	297	316	1
E3T	568	317	298	316	1
E3T	569	318	298	317	1
E3T	570	318	299	298	1
E3T	571	318	319	299	1
E3T	572	319	300	299	1
E3T	573	320	300	319	1
E3T	574	300	320	301	1
E3T	575	320	321	301	1
E3T	576	302	301	321	1
E3T	577	321	303	302	1
E3T	578	303	321	322	1
E3T	579	303	322	323	1
E3T	580	304	303	323	1
E3T	581	323	324	304	1
E3T	582	304	324	305	1
E3T	583	324	325	305	1
E3T	584	306	305	325	1
E3T	585	307	306	325	1
E3T	586	326	307	325	1
E3T	587	327	307	326	1
E3T	588	308	307	327	1
E3T	589	308	327	328	1
E3T	590	308	328	309	1
E3T	591	328	329	309	1
E3T	592	310	309	329	1
E3T	593	312	310	329	1
E3T	594	312	311	310	1
E3T	595	312	329	313	1
E3T	596	314	313	329	1
E3T	597	329	330	314	1
E3T	598	315	331	316	1
E3T	599	332	316	331	1
E3T	600	316	332	333	1
E3T	601	316	333	317	1
E3T	602	333	334	317	1
E3T	603	334	335	317	1
E3T	604	317	335	318	1
E3T	605	336	318	335	1
E3T	606	319	318	336	1
E3T	607	337	319	336	1
E3T	608	319	337	320	1
E3T	609	320	337	338	1
E3T	610	320	338	321	1
E3T	611	339	321	338	1
E3T	612	321	339	322	1
E3T	613	322	339	340	1
E3T	614	322	340	341	1
E3T	615	322	341	324	1
E3T	616	322	324	323	1
E3T	617	342	324	341	1
E3T	618	325	324	342	1
E3T	619	325	342	326	1
E3T	620	342	343	326	1
E3T	621	343	344	326	1
E3T	622	326	344	345	1
E3T	623	345	327	326	1
E3T	624	345	346	327	1
E3T	625	328	327	346	1
E3T	626	328	346	347	1
E3T	627	328	347	348	1
E3T	628	328	348	329	1
E3T	629	330	329	348	1
E3T	630	348	347	330	1
E3T	631	349	332	331	1
E3T	632	332	349	350	1
E3T	633	333	332	350	1
E3T	634	351	333	350	1
E3T	635	334	333	351	1
E3T	636	334	351	352	1
E3T	637	334	352	335	1
E3T	638	335	352	353	1
E3T	639	335	353	336	1
E3T	640	353	354	336	1
E3T	641	337	336	354	1
E3T	642	337	354	355	1
E3T	643	355	356	337	1
E3T	644	337	356	338	1
E3T	645	357	338	356	1
E3T	646	358	338	357	1
E3T	647	339	338	358	1
E3T	648	340	339	358	1
E3T	649	358	359	340	1
E3T	650	360	340	359	1
E3T	651	340	360	361	1
E3T	652	340	361	341	1
E3T	653	362	341	361	1
E3T	654	342	341	362	1
E3T	655	362	343	342	1
E3T	656	363	343	362	1
E3T	657	343	363	344	1
E3T	658	364	344	363	1
E3T	659	365	344	364	1
E3T	660	365	345	344	1
E3T	661	346	345	365	1
E3T	662	366	346	365	1
E3T	663	346	366	347	1
E3T	664	367	350	349	1
E3T	665	350	367	368	1
E3T	666	351	350	368	1
E3T	667	351	368	369	1
E3T	668	351	369	370	1
E3T	669	352	351	370	1
E3T	670	352	370	371	1
E3T	671	371	353	352	1
E3T	672	372	353	371	1
E3T	673	355	353	372	1
E3T	674	353	355	354	1
E3T	675	373	355	372	1
E3T	676	355	373	356	1
E3T	677	373	357	356	1
E3T	678	357	373	374	1
E3T	679	374	375	357	1
E3T	680	358	357	375	1
E3T	681	358	375	359	1
E3T	682	375	376	359	1
E3T	683	360	359	376	1
E3T	684	377	360	376	1
E3T	685	378	360	377	1
E3T	686	378	379	360	1
E3T	687	361	360	379	1
E3T	688	361	379	380	1
E3T	689	363	361	380	1
E3T	690	362	361	363	1
E3T	691	381	363	380	1
E3T	692	381	364	363	1
E3T	693	364	381	382	1

E3T	694	364	382	383	1
E3T	695	365	364	383	1
E3T	696	383	366	365	1
E3T	697	366	383	382	1
E3T	698	368	367	384	1
E3T	699	384	385	368	1
E3T	700	385	369	368	1
E3T	701	369	385	386	1
E3T	702	369	386	387	1
E3T	703	369	387	370	1
E3T	704	387	388	370	1
E3T	705	371	370	388	1
E3T	706	389	371	388	1
E3T	707	389	372	371	1
E3T	708	372	389	390	1
E3T	709	390	391	372	1
E3T	710	372	391	373	1
E3T	711	374	373	391	1
E3T	712	374	391	392	1
E3T	713	374	392	393	1
E3T	714	375	374	393	1
E3T	715	375	393	376	1
E3T	716	394	376	393	1
E3T	717	377	376	394	1
E3T	718	377	394	395	1
E3T	719	395	396	377	1
E3T	720	396	378	377	1
E3T	721	397	378	396	1
E3T	722	398	378	397	1
E3T	723	379	378	398	1
E3T	724	379	398	380	1
E3T	725	380	398	399	1
E3T	726	380	399	381	1
E3T	727	384	400	385	1
E3T	728	385	400	401	1
E3T	729	385	401	386	1
E3T	730	401	402	386	1
E3T	731	403	386	402	1
E3T	732	387	386	403	1
E3T	733	387	403	404	1
E3T	734	388	387	404	1
E3T	735	405	388	404	1
E3T	736	388	405	390	1
E3T	737	389	388	390	1
E3T	738	390	405	406	1
E3T	739	390	406	391	1
E3T	740	391	406	392	1
E3T	741	407	392	406	1
E3T	742	407	393	392	1
E3T	743	393	407	408	1
E3T	744	393	408	409	1
E3T	745	393	409	394	1
E3T	746	410	394	409	1
E3T	747	410	395	394	1
E3T	748	395	410	411	1
E3T	749	412	395	411	1
E3T	750	412	396	395	1
E3T	751	396	412	413	1
E3T	752	396	413	397	1
E3T	753	397	413	414	1
E3T	754	397	414	399	1
E3T	755	398	397	399	1
E3T	756	401	400	415	1
E3T	757	415	416	401	1
E3T	758	401	416	402	1
E3T	759	402	416	417	1
E3T	760	417	418	402	1
E3T	761	403	402	418	1
E3T	762	403	418	419	1
E3T	763	403	419	404	1
E3T	764	420	404	419	1
E3T	765	405	404	420	1
E3T	766	420	421	405	1
E3T	767	421	406	405	1
E3T	768	422	406	421	1
E3T	769	406	422	407	1
E3T	770	407	422	408	1
E3T	771	422	423	408	1
E3T	772	408	423	409	1
E3T	773	409	423	424	1
E3T	774	424	410	409	1
E3T	775	411	410	424	1
E3T	776	411	424	425	1
E3T	777	425	426	411	1
E3T	778	411	426	412	1
E3T	779	412	426	427	1
E3T	780	412	427	413	1
E3T	781	428	413	427	1
E3T	782	414	413	428	1
E3T	783	415	429	430	1
E3T	784	415	430	416	1
E3T	785	430	417	416	1
E3T	786	431	417	430	1
E3T	787	417	431	432	1
E3T	788	418	417	432	1
E3T	789	432	433	418	1
E3T	790	419	418	433	1
E3T	791	419	433	434	1
E3T	792	420	419	434	1
E3T	793	434	435	420	1
E3T	794	436	420	435	1
E3T	795	420	436	421	1
E3T	796	421	436	437	1
E3T	797	421	437	422	1
E3T	798	422	437	423	1
E3T	799	437	438	423	1
E3T	800	424	423	438	1
E3T	801	425	424	438	1
E3T	802	425	438	439	1
E3T	803	425	439	440	1
E3T	804	425	440	441	1
E3T	805	426	425	441	1
E3T	806	441	442	426	1
E3T	807	426	442	443	1
E3T	808	443	427	426	1
E3T	809	427	443	428	1
E3T	810	429	444	445	1
E3T	811	430	429	445	1
E3T	812	445	446	430	1
E3T	813	430	446	431	1
E3T	814	447	431	446	1
E3T	815	431	447	448	1
E3T	816	431	448	432	1
E3T	817	448	449	432	1
E3T	818	432	449	433	1
E3T	819	433	449	450	1
E3T	820	433	450	435	1
E3T	821	435	434	433	1
E3T	822	435	450	451	1
E3T	823	451	436	435	1
E3T	824	452	436	451	1
E3T	825	452	437	436	1
E3T	826	437	452	438	1
E3T	827	438	452	439	1
E3T	828	452	453	439	1
E3T	829	453	454	439	1
E3T	830	454	455	439	1
E3T	831	455	440	439	1
E3T	832	456	440	455	1
E3T	833	440	456	457	1

E3T	834	440	457	441	1
E3T	835	441	457	458	1
E3T	836	458	442	441	1
E3T	837	460	444	459	1
E3T	838	460	445	444	1
E3T	839	460	446	445	1
E3T	840	446	460	461	1
E3T	841	446	461	447	1
E3T	842	447	461	462	1
E3T	843	447	462	463	1
E3T	844	447	463	464	1
E3T	845	464	448	447	1
E3T	846	449	448	464	1
E3T	847	449	464	465	1
E3T	848	465	450	449	1
E3T	849	465	466	450	1
E3T	850	450	466	451	1
E3T	851	451	466	453	1
E3T	852	452	451	453	1
E3T	853	466	454	453	1
E3T	854	467	454	466	1
E3T	855	467	468	454	1
E3T	856	469	454	468	1
E3T	857	454	469	455	1
E3T	858	470	455	469	1
E3T	859	455	470	456	1
E3T	860	470	471	456	1
E3T	861	471	457	456	1
E3T	862	457	471	472	1
E3T	863	472	473	457	1
E3T	864	473	458	457	1
E3T	865	458	473	474	1
E3T	866	459	475	476	1
E3T	867	476	477	459	1
E3T	868	459	477	460	1
E3T	869	460	477	461	1
E3T	870	478	461	477	1
E3T	871	461	478	462	1
E3T	872	462	478	479	1
E3T	873	462	479	480	1
E3T	874	480	463	462	1
E3T	875	480	481	463	1
E3T	876	482	463	481	1
E3T	877	483	463	482	1
E3T	878	463	483	464	1
E3T	879	483	465	464	1
E3T	880	483	467	465	1
E3T	881	467	466	465	1
E3T	882	483	484	467	1
E3T	883	467	484	468	1
E3T	884	468	484	485	1
E3T	885	468	485	469	1
E3T	886	485	486	469	1
E3T	887	486	470	469	1
E3T	888	486	487	470	1
E3T	889	470	487	488	1
E3T	890	470	488	471	1
E3T	891	489	471	488	1
E3T	892	472	471	489	1
E3T	893	472	489	490	1
E3T	894	490	491	472	1
E3T	895	472	491	492	1
E3T	896	493	472	492	1
E3T	897	493	473	472	1
E3T	898	493	474	473	1
E3T	899	475	494	476	1
E3T	900	495	476	494	1
E3T	901	477	476	495	1
E3T	902	478	477	495	1
E3T	903	478	495	496	1
E3T	904	478	496	479	1
E3T	905	479	496	497	1
E3T	906	498	479	497	1
E3T	907	479	498	481	1
E3T	908	479	481	480	1
E3T	909	499	481	498	1
E3T	910	500	481	499	1
E3T	911	481	500	482	1
E3T	912	484	482	500	1
E3T	913	483	482	484	1
E3T	914	501	484	500	1
E3T	915	485	484	501	1
E3T	916	501	502	485	1
E3T	917	486	485	502	1
E3T	918	486	502	503	1
E3T	919	486	503	504	1
E3T	920	486	504	487	1
E3T	921	505	487	504	1
E3T	922	487	505	506	1
E3T	923	506	507	487	1
E3T	924	488	487	507	1
E3T	925	507	508	488	1
E3T	926	488	508	489	1
E3T	927	508	490	489	1
E3T	928	490	508	509	1
E3T	929	509	510	490	1
E3T	930	490	510	491	1
E3T	931	511	491	510	1
E3T	932	492	491	511	1
E3T	933	492	511	512	1
E3T	934	493	492	512	1
E3T	935	495	494	513	1
E3T	936	513	496	495	1
E3T	937	497	496	514	1
E3T	938	497	514	515	1
E3T	939	497	515	498	1
E3T	940	498	515	516	1
E3T	941	516	499	498	1
E3T	942	516	517	499	1
E3T	943	500	499	517	1
E3T	944	500	517	501	1
E3T	945	518	501	517	1
E3T	946	502	501	518	1
E3T	947	502	518	519	1
E3T	948	503	502	519	1
E3T	949	503	519	520	1
E3T	950	520	504	503	1
E3T	951	520	521	504	1
E3T	952	504	521	505	1
E3T	953	522	507	506	1
E3T	954	507	522	523	1
E3T	955	523	508	507	1
E3T	956	523	509	508	1
E3T	957	516	524	517	1
E3T	958	517	524	518	1
E3T	959	518	524	525	1
E3T	960	519	518	525	1
E3T	961	526	519	525	1
E3T	962	519	526	520	1
ND	1	752707.49923672	645018.66174852	0.0	
ND	2	752254.21595463	644882.0660951	0.0	
ND	3	752790.38487465	644665.85875901	0.0	
ND	4	752976.20056827	644816.55497634	0.0	
ND	5	753092.31813746	645134.62585148	0.0	
ND	6	752376.71237875	644476.0369345	0.0	
ND	7	752663.25751453	644317.22353031	0.0	
ND	8	752863.69447488	644351.47590577	0.0	
ND	9	753228.80706613	644433.1263488	0.0	
ND	10	753146.85173953	644852.82994195	0.0	
ND	11	753513.97396106	645015.15093731	0.0	

ND	12	753440.07811452	645239.42235109	0.0
ND	13	752499.20880286	644070.0077739	0.0
ND	14	752905.08791615	644021.28831564	0.0
ND	15	753080.92711694	644179.18138578	0.0
ND	16	753300.90566075	644083.93760677	0.0
ND	17	753427.7999235	644373.81325121	0.0
ND	18	753427.58587832	644721.34686429	0.0
ND	19	753599.65707214	644777.1547432	0.0
ND	20	753679.256186	645041.42304116	0.0
ND	21	753613.95810305	645291.8206009	0.0
ND	22	752621.70522698	643663.9786133	0.0
ND	23	752756.17903872	643815.67382546	0.0
ND	24	752983.2555048	643591.17921853	0.0
ND	25	753153.9893796	643868.91460413	0.0
ND	26	753438.58375183	643854.1152485	0.0
ND	27	753517.53582019	644098.47381097	0.0
ND	28	753810.23780304	644215.55460411	0.0
ND	29	753606.91143326	644506.89973989	0.0
ND	30	753780.29329977	644537.2354029	0.0
ND	31	753786.98730888	644846.36946987	0.0
ND	32	753904.47788504	645137.42110361	0.0
ND	33	753925.39379134	645385.67087736	0.0
ND	34	752744.2016511	643257.9494527	0.0
ND	35	753003.15873236	643183.2700991	0.0
ND	36	753207.71309136	643264.11244954	0.0
ND	37	753283.56570526	643586.69236764	0.0
ND	38	753586.08445157	643507.80925781	0.0
ND	39	753686.04699971	643834.88485555	0.0
ND	40	753742.31956652	643986.98030836	0.0
ND	41	753930.55777132	643851.60619823	0.0
ND	42	754119.76300948	644172.7018905	0.0
ND	43	753980.97985513	644450.66460855	0.0
ND	44	753962.47599787	644790.11796124	0.0
ND	45	754303.2954138	644821.69218984	0.0
ND	46	754326.78182916	645137.012341	0.0
ND	47	754236.82947963	645479.52115382	0.0
ND	48	752866.69807522	642851.92029211	0.0
ND	49	753292.3235519	643010.41011395	0.0
ND	50	753465.94478679	643136.08165678	0.0
ND	51	753682.6989108	643092.50645379	0.0
ND	52	753788.44991085	643458.77587903	0.0
ND	53	754043.59384737	643413.21446179	0.0
ND	54	754286.34562612	643810.97948806	0.0
ND	55	754400.05769746	644164.30724525	0.0
ND	56	754362.29090689	644497.88749451	0.0
ND	57	754554.26544046	644829.43816054	0.0
ND	58	754554.05052978	645210.34144848	0.0
ND	59	754407.14278926	645530.84459489	0.0
ND	60	752989.19449933	642445.89113151	0.0
ND	61	753104.23010074	642598.69631517	0.0
ND	62	753235.22385367	642690.68138922	0.0
ND	63	753482.60397704	642758.56511835	0.0
ND	64	753756.6150942	642742.87963606	0.0
ND	65	753892.29443974	643078.11122419	0.0
ND	66	754210.39597099	643048.28920564	0.0
ND	67	754560.15602299	643542.55415666	0.0
ND	68	754660.76367713	643875.18948137	0.0
ND	69	754834.54320017	644216.71028954	0.0
ND	70	754593.22573304	644447.93237384	0.0
ND	71	754835.11439514	644535.57910453	0.0
ND	72	754809.52994513	644960.63852546	0.0
ND	73	754772.88005975	645370.05635394	0.0
ND	74	754706.37829462	645621.01838023	0.0
ND	75	753111.69092345	642039.86197091	0.0
ND	76	753350.2369046	642423.19623603	0.0
ND	77	753580.00499165	642415.4841389	0.0
ND	78	753804.24839446	642401.52439613	0.0
ND	79	753946.72266533	642731.21440434	0.0
ND	80	754068.21489167	642891.90247992	0.0
ND	81	754240.00103042	642614.50901114	0.0
ND	82	754745.25783278	642740.44631421	0.0
ND	83	754618.227179	643136.05606456	0.0
ND	84	754727.84261848	643382.84037345	0.0
ND	85	754846.88235581	643596.99586542	0.0
ND	86	754992.09151548	643931.44668778	0.0
ND	87	755400.57077183	644193.45399083	0.0
ND	88	755312.30190738	644577.20254848	0.0
ND	89	755140.29248706	644931.86253704	0.0
ND	90	755021.57270629	645307.80175205	0.0
ND	91	754958.79629056	645697.08383963	0.0
ND	92	753234.18734757	641633.83281031	0.0
ND	93	753333.46991684	641902.8875001	0.0
ND	94	753432.80280078	642076.12391913	0.0
ND	95	753706.11117484	642082.91586683	0.0
ND	96	753942.67829122	642019.40456167	0.0
ND	97	753996.67150468	642426.99715241	0.0
ND	98	754310.39597487	642039.72118917	0.0
ND	99	754649.87627353	642400.11394389	0.0
ND	100	754957.26762715	642414.78028536	0.0
ND	101	754987.66191491	642827.11909647	0.0
ND	102	754886.80627557	643259.45727109	0.0
ND	103	755077.26734799	643563.52508975	0.0
ND	104	755229.89017359	643813.32667261	0.0
ND	105	755508.73857378	643778.82018067	0.0
ND	106	755769.64030366	644144.90734701	0.0
ND	107	755702.00468684	644575.29124926	0.0
ND	108	755500.30751346	644906.28990921	0.0
ND	109	755452.51331581	645247.47345189	0.0
ND	110	755395.14469166	645555.60394393	0.0
ND	111	755322.93635441	645806.81643274	0.0
ND	112	753319.60906882	641350.69222051	0.0
ND	113	753464.56486431	641549.60071017	0.0
ND	114	753591.92438645	641815.37950401	0.0
ND	115	754146.29789803	641516.62997361	0.0
ND	116	754738.59819058	641790.40846935	0.0
ND	117	754923.67230643	641835.0815318	0.0
ND	118	755275.55646293	642292.07732174	0.0
ND	119	755310.57845525	642573.53589008	0.0
ND	120	755312.14880537	642907.66572843	0.0
ND	121	755183.80462113	643213.08786213	0.0
ND	122	755354.78968901	643482.11295482	0.0
ND	123	755680.88468714	643460.90587807	0.0
ND	124	755843.10007748	643788.73411746	0.0
ND	125	756158.9856658	643911.73640451	0.0
ND	126	756071.75620907	644336.18659992	0.0
ND	127	756071.03679087	644708.39143657	0.0
ND	128	755878.60489579	645060.92554459	0.0
ND	129	755836.67886757	645531.49852382	0.0
ND	130	755687.07641827	645916.54902585	0.0
ND	131	753428.20353499	640990.74277494	0.0
ND	132	753620.48409734	641436.96333471	0.0
ND	133	753970.95464325	641201.04637841	0.0
ND	134	754257.04218388	641125.6664307	0.0
ND	135	754840.7080476	641401.11463947	0.0
ND	136	755064.07335983	641388.35090734	0.0
ND	137	755475.48682308	641874.10132352	0.0
ND	138	755658.59987847	642393.20602779	0.0
ND	139	755590.92908469	642790.64287523	0.0
ND	140	755499.65032205	643150.59526323	0.0
ND	141	755832.57014284	643097.11336378	0.0
ND	142	756014.49783848	643488.20276166	0.0
ND	143	756337.4693939	643519.7411314	0.0
ND	144	756564.89382133	643778.33129133	0.0
ND	145	756432.83527528	644153.63123772	0.0
ND	146	756393.80435274	644541.25397353	0.0
ND	147	756415.11492343	644945.19246192	0.0
ND	148	756188.75354841	645286.25750507	0.0
ND	149	756218.20279919	645672.51660656	0.0
ND	150	756051.21648212	646026.28161896	0.0
ND	151	753554.25242419	640572.9385407	0.0

ND	152	753761.66532011	641093.35924394	0.0
ND	153	754030.8918765	640759.518314	0.0
ND	154	754312.07090859	640655.21028151	0.0
ND	155	754658.19407321	640781.25416416	0.0
ND	156	754974.72723494	640922.4746847	0.0
ND	157	755230.00187748	640935.23841682	0.0
ND	158	755728.01506074	641138.34764019	0.0
ND	159	755632.81419198	641521.73000264	0.0
ND	160	755792.09086394	641667.35438843	0.0
ND	161	755857.57127353	641878.80681147	0.0
ND	162	755997.33097858	642125.44957252	0.0
ND	163	756051.02893228	642437.94420334	0.0
ND	164	755847.84010738	642711.71418489	0.0
ND	165	756125.57932851	643125.48293215	0.0
ND	166	756468.54642114	643143.23761884	0.0
ND	167	756735.16115549	643428.02300409	0.0
ND	168	757167.54890878	643829.24345476	0.0
ND	169	756940.7806234	644240.33686565	0.0
ND	170	757124.19349214	644721.65035054	0.0
ND	171	756993.17293917	645335.53152158	0.0
ND	172	756576.61141015	645502.15613319	0.0
ND	173	756516.36621616	645824.40971414	0.0
ND	174	756463.14602161	646150.41543733	0.0
ND	175	753680.30131339	640155.13430646	0.0
ND	176	753801.42801151	640546.86878156	0.0
ND	177	754095.49650643	640514.83230581	0.0
ND	178	754255.66153487	640243.42185334	0.0
ND	179	754635.2900729	640289.21939058	0.0
ND	180	755070.45522589	640514.03525662	0.0
ND	181	755427.83972546	640520.41712269	0.0
ND	182	755680.51593628	640788.70985669	0.0
ND	183	755946.78487613	640943.17049141	0.0
ND	184	755933.16448768	641289.64113777	0.0
ND	185	756124.32993542	641649.82065502	0.0
ND	186	756193.25586392	641864.70472062	0.0
ND	187	756289.86669551	642171.94687612	0.0
ND	188	756421.20406198	642497.781217	0.0
ND	189	756242.29582232	642781.77629791	0.0
ND	190	756664.75744542	642753.56884996	0.0
ND	191	756774.17062442	643093.94903816	0.0
ND	192	756987.1193755	643267.22307144	0.0
ND	193	757428.33303779	643296.24467534	0.0
ND	194	757465.9663299	643835.94946423	0.0
ND	195	757223.96188626	644204.29561402	0.0
ND	196	757463.98194409	644663.42589643	0.0
ND	197	757261.39078604	645335.21313826	0.0
ND	198	757080.87819799	645933.78839102	0.0
ND	199	756703.49349037	645850.48482612	0.0
ND	200	756663.07791231	646210.66435523	0.0
ND	201	753806.35020258	639737.33007221	0.0
ND	202	753986.85465781	639929.08467246	0.0
ND	203	754018.42761367	640186.1058021	0.0
ND	204	754307.2231606	639994.964572	0.0
ND	205	754659.07633322	639813.73526141	0.0
ND	206	755042.62915997	640079.60201885	0.0
ND	207	755485.27652003	640060.9227661	0.0
ND	208	755819.71857575	640438.95277293	0.0
ND	209	756084.14041181	640739.24556524	0.0
ND	210	756223.39853447	641135.77553058	0.0
ND	211	756358.90278528	641582.58235785	0.0
ND	212	756532.86358966	641898.34116089	0.0
ND	213	756586.08278834	642206.13184459	0.0
ND	214	756812.67243372	642392.47065648	0.0
ND	215	757087.62720567	642515.80462442	0.0
ND	216	756948.84425815	642879.36797633	0.0
ND	217	757007.09777059	643086.6416627	0.0
ND	218	757392.28119708	642845.5732455	0.0
ND	219	757680.69205698	642946.40458173	0.0
ND	220	757842.78234071	643407.33122009	0.0
ND	221	757672.13038748	643973.20981006	0.0
ND	222	756969.53102243	646303.01314565	0.0
ND	223	753932.39909178	639319.52583797	0.0
ND	224	754204.3664774	639673.15166211	0.0
ND	225	754476.3583476	639460.06374584	0.0
ND	226	755119.92505435	639434.55975469	0.0
ND	227	755861.80661779	639607.81027558	0.0
ND	228	755982.44973937	640074.62811085	0.0
ND	229	756230.83516347	640417.13105169	0.0
ND	230	756424.32162901	640804.16547671	0.0
ND	231	756679.19408179	641272.6705425	0.0
ND	232	756580.11471461	641653.90841088	0.0
ND	233	756838.69510785	641754.53149918	0.0
ND	234	756878.64317902	642043.91666825	0.0
ND	235	757184.17771179	642202.39324019	0.0
ND	236	757580.34605516	642517.16809495	0.0
ND	237	757814.03765452	642543.21013586	0.0
ND	238	758066.11580616	642666.76267686	0.0
ND	239	757954.44907344	643037.04694848	0.0
ND	240	754058.44798098	638901.72160373	0.0
ND	241	754149.87275901	639284.11366943	0.0
ND	242	754426.69667526	639084.70972835	0.0
ND	243	754806.03521217	638992.15360704	0.0
ND	244	755219.41635856	638896.58545404	0.0
ND	245	755575.25811943	639153.92033219	0.0
ND	246	755958.3241628	639139.05212856	0.0
ND	247	756242.3429293	639349.67430729	0.0
ND	248	756216.88985183	639722.62981329	0.0
ND	249	756379.18018056	640033.06912413	0.0
ND	250	756601.85986332	640382.15342562	0.0
ND	251	756712.40464307	640827.64902139	0.0
ND	252	757030.46554785	640966.89243922	0.0
ND	253	757002.0480291	641416.56258065	0.0
ND	254	757117.3455383	641813.82922505	0.0
ND	255	757423.27650633	642000.55659545	0.0
ND	256	757814.03765452	642215.93869171	0.0
ND	257	758177.78253889	642296.47840525	0.0
ND	258	754178.25886846	638504.59397798	0.0
ND	259	754473.31098907	638692.51910003	0.0
ND	260	754907.00210353	638504.84460384	0.0
ND	261	755325.95447353	638510.24048918	0.0
ND	262	755621.85687161	638704.08054026	0.0
ND	263	755861.38475315	638895.26473823	0.0
ND	264	756139.02544377	638976.00391668	0.0
ND	265	756411.83827693	639038.68804815	0.0
ND	266	756569.72030269	639223.62796928	0.0
ND	267	756638.25109993	639682.85490965	0.0
ND	268	756738.60157077	640008.56146282	0.0
ND	269	757051.15236809	640196.64835713	0.0
ND	270	756881.18616257	640524.90232805	0.0
ND	271	757383.18662343	640884.2495755	0.0
ND	272	757339.91940064	641241.20416357	0.0
ND	273	757362.38692733	641660.5400444	0.0
ND	274	757782.0166112	641719.75969849	0.0
ND	275	758119.84780731	641719.9172222	0.0
ND	276	758332.30311304	641784.09140982	0.0
ND	277	754298.06975593	638107.46635222	0.0
ND	278	754573.50991988	638297.362148	0.0
ND	279	754768.15681243	637994.49954979	0.0
ND	280	755130.78683203	638078.98723722	0.0
ND	281	755441.41603487	638126.46709485	0.0
ND	282	755784.34876311	638292.51007676	0.0
ND	283	756006.40855717	638625.25620446	0.0
ND	284	756291.72965523	638544.08302751	0.0
ND	285	756435.0	638817.0	0.0
ND	286	756733.05462036	638960.87276259	0.0
ND	287	756811.17103316	639259.13542965	0.0
ND	288	757084.36292937	639791.47950955	0.0
ND	289	757647.32443877	640043.35595043	0.0
ND	290	757569.21915208	640479.44380112	0.0
ND	291	757575.18492459	640935.62940257	0.0

ND	292	757590.75223872	641240.87331385	0.0
ND	293	757924.37485326	641155.27451597	0.0
ND	294	758259.82169168	641234.50122382	0.0
ND	295	758455.91951357	641374.18200841	0.0
ND	296	754417.88064341	637710.33872647	0.0
ND	297	754970.05754841	637626.73645892	0.0
ND	298	755563.20097286	637744.66931635	0.0
ND	299	755806.7795074	637906.92961881	0.0
ND	300	756200.0	638311.0	0.0
ND	301	756555.75192819	638414.05619811	0.0
ND	302	756710.26322222	638546.49445013	0.0
ND	303	756904.57124641	638620.26252647	0.0
ND	304	757068.77759149	639109.20257278	0.0
ND	305	757214.17002989	639396.79987197	0.0
ND	306	757577.52612022	639704.0552249	0.0
ND	307	757911.90230444	639734.93539852	0.0
ND	308	758017.68227061	640011.0599384	0.0
ND	309	758007.68720646	640304.72802252	0.0
ND	310	757834.20514367	640601.71013248	0.0
ND	311	757784.83386536	640964.63761278	0.0
ND	312	758021.92460548	640933.19239534	0.0
ND	313	758297.38058459	640936.7243477	0.0
ND	314	758564.10854384	641015.42959323	0.0
ND	315	754537.69153089	637313.21110072	0.0
ND	316	755102.81664123	637263.68381241	0.0
ND	317	755708.25978995	637371.0916598	0.0
ND	318	755932.84270461	637527.36081043	0.0
ND	319	756262.09996737	637924.6484495	0.0
ND	320	756419.94744708	638003.57218935	0.0
ND	321	756946.9057605	638117.03103669	0.0
ND	322	757312.94461394	638364.34525224	0.0
ND	323	757197.76099179	638736.58386078	0.0
ND	324	757465.7756363	638855.56523509	0.0
ND	325	757620.74112946	639330.15035038	0.0
ND	326	758065.30975348	639305.052855	0.0
ND	327	758122.03282384	639739.18468965	0.0
ND	328	758450.98439253	640106.64128882	0.0
ND	329	758374.51931219	640571.80386088	0.0
ND	330	758697.7431145	640572.30033274	0.0
ND	331	754657.50241836	636916.08347496	0.0
ND	332	755137.22414778	636872.2619316	0.0
ND	333	755490.36560779	636873.72097478	0.0
ND	334	755830.46372152	636989.5517541	0.0
ND	335	756080.23892112	637154.71487138	0.0
ND	336	756335.38629724	637524.39234025	0.0
ND	337	756504.50859692	637608.95349009	0.0
ND	338	756907.04579434	637757.28065831	0.0
ND	339	757225.06789871	638006.2131756	0.0
ND	340	757737.4250402	638038.77027154	0.0
ND	341	757755.47525996	638467.51915211	0.0
ND	342	757792.57908116	638952.77188347	0.0
ND	343	758231.44785684	638893.53103346	0.0
ND	344	758492.81510253	639061.55723945	0.0
ND	345	758302.07133068	639409.84595762	0.0
ND	346	758577.33874808	639724.40056505	0.0
ND	347	758831.37768516	640129.17107226	0.0
ND	348	758599.54466353	640285.69988486	0.0
ND	349	754777.31330585	636518.95584922	0.0
ND	350	755218.23324229	636488.16090336	0.0
ND	351	755891.98442708	636593.53559757	0.0
ND	352	756225.06442986	636781.03686813	0.0
ND	353	756469.2571227	637105.2761238	0.0
ND	354	756481.90757168	637386.81581065	0.0
ND	355	756636.91314633	637193.55005671	0.0
ND	356	756791.4168756	637466.28125915	0.0
ND	357	756967.20784728	637457.31445893	0.0
ND	358	757416.10480686	637665.22308832	0.0
ND	359	757809.11163556	637636.36986677	0.0
ND	360	758243.92517055	637804.28448621	0.0
ND	361	758225.26918797	638332.14226007	0.0
ND	362	758147.22785893	638653.84613517	0.0
ND	363	758685.39498014	638707.21808107	0.0
ND	364	758884.28651445	639017.01389399	0.0
ND	365	758769.58889394	639367.47884554	0.0
ND	366	758965.01225581	639686.04181177	0.0
ND	367	754897.12419332	636121.82822346	0.0
ND	368	755369.25360916	636126.14110735	0.0
ND	369	755957.75640157	636198.21104075	0.0
ND	370	756369.06759141	636407.03535797	0.0
ND	371	756594.70715675	636673.14343184	0.0
ND	372	756752.55463646	636847.90314151	0.0
ND	373	756937.40571914	637073.93685802	0.0
ND	374	757150.95134146	637111.62818648	0.0
ND	375	757543.21150116	637291.97031204	0.0
ND	376	757967.73837713	637291.29695972	0.0
ND	377	758383.59028731	637385.10000419	0.0
ND	378	758820.42713869	637655.20539144	0.0
ND	379	758580.73561068	638025.63229079	0.0
ND	380	758721.2193466	638402.38412803	0.0
ND	381	759232.28139713	638799.7832908	0.0
ND	382	759072.12630571	639330.85400757	0.0
ND	383	758921.6141361	639347.44928897	0.0
ND	384	755016.9350808	635724.70059771	0.0
ND	385	755587.45512662	635799.08189413	0.0
ND	386	756037.54002648	635805.46697639	0.0
ND	387	756507.45397482	636030.92781792	0.0
ND	388	756735.64240649	636284.16214257	0.0
ND	389	756755.16141567	636537.01396202	0.0
ND	390	756910.40211616	636413.82257232	0.0
ND	391	757079.52441584	636650.59379188	0.0
ND	392	757225.28321809	636647.49249469	0.0
ND	393	757653.37361326	636874.48547038	0.0
ND	394	758143.55823518	636914.24993712	0.0
ND	395	758626.49930127	636930.25337391	0.0
ND	396	758933.66177237	637270.15969388	0.0
ND	397	759213.93419876	637612.19262846	0.0
ND	398	758986.64781281	637936.86182591	0.0
ND	399	759422.71466612	638168.31081145	0.0
ND	400	755136.74596828	635327.57297196	0.0
ND	401	755801.62641071	635469.36612441	0.0
ND	402	756122.22245808	635413.75915367	0.0
ND	403	756521.37314036	635645.01292189	0.0
ND	404	756857.03239011	635881.82942854	0.0
ND	405	757025.30524448	636129.08750026	0.0
ND	406	757127.17068217	636289.45972605	0.0
ND	407	757400.09277573	636509.27098399	0.0
ND	408	757684.32300891	636447.09306728	0.0
ND	409	758001.77884573	636509.07299348	0.0
ND	410	758356.89305458	636580.35914286	0.0
ND	411	758734.52621145	636522.40944777	0.0
ND	412	759134.80731541	636876.07862996	0.0
ND	413	759426.42015389	637239.32783199	0.0
ND	414	759616.82923314	637524.63122983	0.0
ND	415	755256.55685575	634930.4453462	0.0
ND	416	755957.18239854	635108.97940768	0.0
ND	417	756223.04741871	635026.05503052	0.0
ND	418	756497.66660381	635253.91925121	0.0
ND	419	756932.95175612	635534.38661397	0.0
ND	420	757170.20239752	635657.59710554	0.0
ND	421	757335.04735894	635940.123587	0.0
ND	422	757456.02644576	636139.97983351	0.0
ND	423	757882.03230159	636124.65118867	0.0
ND	424	758375.45536411	636193.85134205	0.0
ND	425	758941.30248018	635973.53992498	0.0
ND	426	759321.52773144	636338.22324789	0.0
ND	427	759569.82352917	636911.07726756	0.0
ND	428	759751.36684933	637078.50749046	0.0
ND	429	755376.36774323	634533.31772045	0.0
ND	430	755984.6060006	634740.8919843	0.0
ND	431	756506.09700322	634600.27373533	0.0

ND	432	756682.66947547	634910.94484928	0.0
ND	433	757056.21250344	635122.88451396	0.0
ND	434	757106.78960185	635419.85526249	0.0
ND	435	757282.47117547	635246.87870451	0.0
ND	436	757428.55014558	635651.48454995	0.0
ND	437	757788.34777791	635893.42981109	0.0
ND	438	758168.28901709	635810.59585514	0.0
ND	439	758364.1231465	635351.60961435	0.0
ND	440	759025.95508176	635284.22588353	0.0
ND	441	759460.72020553	635734.77035927	0.0
ND	442	760022.10934467	636180.73140491	0.0
ND	443	759874.34707303	636670.70780724	0.0
ND	444	755560.78899375	633922.03125977	0.0
ND	445	755808.20814623	634121.78006663	0.0
ND	446	756253.17154727	634198.25815119	0.0
ND	447	756832.93791986	634262.87631069	0.0
ND	448	756844.20176932	634623.19609235	0.0
ND	449	757133.25568348	634813.70560713	0.0
ND	450	757333.72607651	634895.81851301	0.0
ND	451	757485.46488528	635236.82001786	0.0
ND	452	757764.69536043	635505.47962083	0.0
ND	453	757864.13614992	635127.27428048	0.0
ND	454	758131.05615075	634752.12381644	0.0
ND	455	758669.41905946	634728.39305575	0.0
ND	456	759133.06707449	634759.90474387	0.0
ND	457	759748.05335924	634864.83100462	0.0
ND	458	760197.52333123	635599.06253163	0.0
ND	459	755707.32919818	633436.30609165	0.0
ND	460	755988.65850276	633664.15459153	0.0
ND	461	756504.03230562	633743.6875858	0.0
ND	462	756964.73375878	633674.44647702	0.0
ND	463	757122.57095089	634132.33747981	0.0
ND	464	757207.88350364	634473.12628622	0.0
ND	465	757365.64325492	634569.53502311	0.0
ND	466	757597.82507563	634810.06061416	0.0
ND	467	757750.10447384	634446.67410824	0.0
ND	468	758082.98957922	634394.81350686	0.0
ND	469	758540.71797666	634482.32040637	0.0
ND	470	759014.55998639	634272.69225793	0.0
ND	471	759497.42117678	634368.36429721	0.0
ND	472	759950.24849592	634292.04894598	0.0
ND	473	760141.28141504	634768.71428036	0.0
ND	474	760425.08147988	634844.48477807	0.0
ND	475	755875.29884923	632879.55044012	0.0
ND	476	756079.69493301	632969.54550292	0.0
ND	477	756186.04780694	633381.17514451	0.0
ND	478	756679.00489301	633129.69287005	0.0
ND	479	757111.75903599	633122.10760347	0.0
ND	480	757154.64421994	633637.2507409	0.0
ND	481	757377.95981747	633628.41688308	0.0
ND	482	757532.74208827	633926.48721985	0.0
ND	483	757505.57918814	634175.21991828	0.0
ND	484	757852.19754287	634067.53562001	0.0
ND	485	758332.38523505	634146.21934434	0.0
ND	486	758610.93701216	634010.91100503	0.0
ND	487	759022.66842027	633710.82097095	0.0
ND	488	759302.48013902	634027.00465461	0.0
ND	489	759598.72939919	634054.83004897	0.0
ND	490	759790.45830704	633838.62511032	0.0
ND	491	760089.21613342	633848.55726344	0.0
ND	492	760349.65834876	633915.89340005	0.0
ND	493	760594.72337863	634281.95758106	0.0
ND	494	756043.26850027	632322.79478859	0.0
ND	495	756454.71467437	632845.45734594	0.0
ND	496	756830.63380256	632561.40741988	0.0
ND	497	757285.89506207	632887.33847792	0.0
ND	498	757587.6155359	633132.89955587	0.0
ND	499	757869.08988999	633361.34250991	0.0
ND	500	757828.29650534	633728.48297177	0.0
ND	501	758123.32707456	633768.28530959	0.0
ND	502	758330.20669904	633737.47345062	0.0
ND	503	758595.21213678	633528.59538698	0.0
ND	504	758774.77780696	633548.20060269	0.0
ND	505	759070.31908047	633240.14852756	0.0
ND	506	759255.88356274	633296.38421544	0.0
ND	507	759280.10776031	633677.04179117	0.0
ND	508	759525.66279348	633812.34762578	0.0
ND	509	759775.35973844	633453.8129464	0.0
ND	510	759946.40951541	633505.64866306	0.0
ND	511	760428.41542267	633651.71796569	0.0
ND	512	760754.94138176	633750.67668885	0.0
ND	513	756555.56023719	632478.04558922	0.0
ND	514	757343.56045454	632716.85086872	0.0
ND	515	757673.47526439	632816.83221239	0.0
ND	516	758009.63450816	632918.70575616	0.0
ND	517	758092.51521559	633398.54300201	0.0
ND	518	758225.27377999	633419.77234861	0.0
ND	519	758391.24521352	633422.53258689	0.0
ND	520	758746.70683495	633142.07695105	0.0
ND	521	758873.57275344	633180.52260328	0.0
ND	522	759393.36341371	633338.04769622	0.0
ND	523	759640.08158182	633412.81669038	0.0
ND	524	758232.1961503	632986.15369551	0.0
ND	525	758333.08258601	633016.72748526	0.0
ND	526	758491.30965475	633064.67844218	0.0

Appendix B. Hydrodynamic model (RSM HSE) xml input file

```
<?xml version="1.0" ?>
<!DOCTYPE hse SYSTEM "../hse.dtd" [ ]>
<hse>
  <control
    tslen="6"
    tstype="hour"
    startdate="1jan2002"
    starttime="1200"
    enddate="31dec2004"
    endtime="1200"
    alpha="0.5000"
    solver="PETSC"
    method="gmres"
    precond="ilu"
    waterquality="false"
    waterqual_file="RASwq.xml">
  </control>
  <mesh>
    <geometry file="RAS_6.2dm" mult="0.3048"> </geometry>
    <shead> <gms file="ras_initial_head.dat" /> </shead>
    <bottom> <gms file="bottom_elev.dat"/> </bottom>
    <surface> <gms file="ras_bathy.dat"/> </surface>

    <rain>
      <indexed file="rain.index">
        <entry id="1">
      <dss file="Rain_ET.dss" pn="/RAS/WCA3A/RAINFALL//1DAY/OBS/"
         units="METERS" type="PER-CUM">
          </dss>
        </entry>
      </indexed>
    </rain>
    <refet>
      <indexed file="refet.index">
        <entry id="1">
      <dss file="Rain_ET.dss" pn="/RAS/WCA3A/PET//1DAY/OBS/"
        units="METERS" type="PER-CUM">
          </dss>
        </entry>
      </indexed>
    </refet>

    <hpModules>
      <indexed file="hp.index">
        <hpmEntry id="1">
          <layer1nsm kw="1.0" rd="0.5" xd="1.0" pd="2.0" kveg="0.00"
imax="0.0">
             <ampmod para="kveg">
                 1  0.830
                31  0.830
                32  0.800
                59  0.800
                60  0.840
                90  0.840
```

```
                 91  0.870
                120  0.870
                121  0.890
                151  0.890
                152  0.900
                181  0.900
                182  0.910
                212  0.910
                213  0.960
                243  0.960
                244  0.960
                273  0.960
                274  0.880
                304  0.880
                305  0.860
                334  0.860
                335  0.840
                365  0.840
              </ampmod>
            </layer1nsm>
          </hpmEntry>
          <hpmEntry id="2">
            <layer1nsm kw="1.0" rd="0.5" xd="1.0" pd="1.0" kveg="0.00"
imax="0.0">
              <ampmod para="kveg">
                  1  0.830
                 31  0.830
                 32  0.800
                 59  0.800
                 60  0.840
                 90  0.840
                 91  0.870
                120  0.870
                121  0.890
                151  0.890
                152  0.900
                181  0.900
                182  0.910
                212  0.910
                213  0.960
                243  0.960
                244  0.960
                273  0.960
                274  0.880
                304  0.880
                305  0.860
                334  0.860
                335  0.840
                365  0.840
              </ampmod>
            </layer1nsm>
          </hpmEntry>
        </indexed>
      </hpModules>

      <mesh_bc>
        <noflow section="ol">
```

```
        <nodelist> 2 6 13 22 34 48 60 75 92 112 131 151 175 201 223 240 258
277 296 315 331 349 367 384 400 415 429 444 459 475 494 </nodelist>
      </noflow>
      <noflow section="ol">
        <nodelist> 222 198 197 196 221 220 239 238 257 276 295 314 330 347
366 382 381 399 414 428 443 442 458 474 493 512 </nodelist>
      </noflow>

      <wallhead section="ol">
        <nodelist> 2 1 5 12 21 33 47 59 74 91 111 130 150 174 200 222
</nodelist>
        <uniform> <dss file="boundary.dss" pn="/RAS/UPPER/STAGE//1DAY/OBS/"
         units="METERS" type="INST-VAL"/> </uniform>
      </wallhead>
      <wallhead section="ol">
        <nodelist> 494 513 496 514 515 516 524 525 526 520 521 505 506 522
523 509 510 511 512</nodelist>
        <uniform> <dss file="boundary.dss" pn="/RAS/DOWN/STAGE//1DAY/OBS/"
         units="METERS" type="INST-VAL"/> </uniform>
      </wallhead>
    </mesh_bc>

    <conveyance>
      <indexed file="kadlec.index">
        <entry id="1" label="type1">
          <kadlec K="0.19" alpha="0.5" beta="1.67" detent="0.03">
          </kadlec>
        </entry>
        <entry id="2" label="type2">
          <kadlec K="0.17" alpha="0.5" beta="1.67" detent="0.03">
          </kadlec>
        </entry>
      </indexed>
    </conveyance>

    <transmissivity>
      <unconfined k="0.0000035"/>
    </transmissivity>
    <svconverter>
      <constsv sc="0.2"/>
    </svconverter>
  </mesh>

  <output>
    <budgetpackage file="output/budget.nc" dbintl="43200"> </budgetpackage>
    <psbudgetpackage file="output/pseudo.nc" dbintl="43200">
</psbudgetpackage>
    <globalmonitor attr="head">
      <gms file="output/heads.dat"> </gms>
    </globalmonitor>
    <cellmonitor id="161" attr="ponding">
       <dss file="output/ras.dss" pn="/HSE/CELL161/PONDING//1DAY/CALC/">
</dss>
    </cellmonitor>
    <cellmonitor id="224" attr="ponding">
       <dss file="output/ras.dss" pn="/HSE/CELL224/PONDING//1DAY/CALC/">
</dss>
```

```
    </cellmonitor>
    <cellmonitor id="225" attr="ponding">
       <dss file="output/ras.dss" pn="/HSE/CELL225/PONDING//1DAY/CALC/">
</dss>
    </cellmonitor>
    <cellmonitor id="369" attr="ponding">
       <dss file="output/ras.dss" pn="/HSE/CELL369/PONDING//1DAY/CALC/">
</dss>
    </cellmonitor>
    <cellmonitor id="370" attr="ponding">
       <dss file="output/ras.dss" pn="/HSE/CELL370/PONDING//1DAY/CALC/">
</dss>
    </cellmonitor>
    <cellmonitor id="422" attr="ponding">
       <dss file="output/ras.dss" pn="/HSE/CELL422/PONDING//1DAY/CALC/">
</dss>
    </cellmonitor>
    <cellmonitor id="455" attr="ponding">
       <dss file="output/ras.dss" pn="/HSE/CELL455/PONDING//1DAY/CALC/">
</dss>
    </cellmonitor>
    <cellmonitor id="227" attr="ponding">
       <dss file="output/ras.dss" pn="/HSE/CELL227/PONDING//1DAY/CALC/">
</dss>
    </cellmonitor>
    <cellmonitor id="228" attr="ponding">
       <dss file="output/ras.dss" pn="/HSE/CELL228/PONDING//1DAY/CALC/">
</dss>
    </cellmonitor>
    <cellmonitor id="270" attr="ponding">
       <dss file="output/ras.dss" pn="/HSE/CELL270/PONDING//1DAY/CALC/">
</dss>
    </cellmonitor>
    <cellmonitor id="271" attr="ponding">
       <dss file="output/ras.dss" pn="/HSE/CELL271/PONDING//1DAY/CALC/">
</dss>
    </cellmonitor>
    <cellmonitor id="417" attr="ponding">
       <dss file="output/ras.dss" pn="/HSE/CELL417/PONDING//1DAY/CALC/">
</dss>
    </cellmonitor>
    <cellmonitor id="453" attr="ponding">
       <dss file="output/ras.dss" pn="/HSE/CELL453/PONDING//1DAY/CALC/">
</dss>
    </cellmonitor>
    <cellmonitor id="794" attr="head">
       <dss file="output/ras.dss" pn="/HSE/CELL794/HEAD//1DAY/CALC/"> </dss>
    </cellmonitor>
  </output>
</hse>
```

Appendix C. Dry season transport model under current flow regime (RSM HSE) xml input file


```
<?xml version="1.0" ?>
<!DOCTYPE hse SYSTEM "../hse.dtd" [ ]>
<hse>
  <control
    tslen="10"
    tstype="minute"
    startdate="1mar2002"
    starttime="0000"
    enddate="31mar2002"
    endtime="2400"
    alpha="0.5000"
    solver="PETSC"
    method="gmres"
    precond="ilu"
    waterquality="true"
    waterqual_file="RASwq_dry.xml">
  </control>
  <mesh>
    <geometry file="RAS_6.2dm" mult="0.3048"> </geometry>
    <shead> <gms file="ras_initial_head_dry.dat"/> </shead>
    <bottom> <gms file="bottom_elev.dat"/> </bottom>
    <surface> <gms file="ras_bathy.dat"/> </surface>

    <mesh_bc>
      <noflow section="ol">
        <nodelist> 2 6 13 22 34 48 60 75 92 112 131 151 175 201 223 240 258
277 296 315 331 349 367 384 400 415 429 444 459 475 494 </nodelist>
      </noflow>
      <noflow section="ol">
        <nodelist> 222 198 197 196 221 220 239 238 257 276 295 314 330 347
366 382 381 399 414 428 443 442 458 474 493 512 </nodelist>
      </noflow>

      <wallhead section="ol">
        <nodelist> 2 1 5 12 21 33 47 59 74 91 111 130 150 174 200 222
</nodelist>
        <uniform> <dss file="boundary.dss" pn="/RAS/UPPER/STAGE//1DAY/OBS/"
         units="METERS" type="INST-VAL"/> </uniform>
      </wallhead>
      <wallhead section="ol">
        <nodelist> 494 513 496 514 515 516 524 525 526 520 521 505 506 522
523 509 510 511 512</nodelist>
        <uniform> <dss file="boundary.dss" pn="/RAS/DOWN/STAGE//1DAY/OBS/"
         units="METERS" type="INST-VAL"/> </uniform>
      </wallhead>
      <well label="Well1" cellid="86">
        <const value="0.0001"></const>
      </well>
    </mesh_bc>

    <conveyance>
      <indexed file="mannings.index">
        <entry id="1" label="type1">
```

```
          <mannings a="0.19" b="-0.77" detent="0.03"/>
        </entry>
        <entry id="2" label="type2">
          <mannings a="0.17" b="-0.77" detent="0.03"/>
        </entry>
      </indexed>
    </conveyance>

    <transmissivity>
      <unconfined k="0.0000035"/>
    </transmissivity>
    <svconverter>
      <constsv sc="0.2"/>
    </svconverter>
  </mesh>

  <output>
    <budgetpackage file="output/budget.nc" dbintl="1440"> </budgetpackage>
    <psbudgetpackage file="output/pseudo.nc" dbintl="1440">
</psbudgetpackage>
    <globalmonitor attr="head">
      <gms file="output/heads.dat"> </gms>
    </globalmonitor>
    <cellmonitor id="161" attr="ponding">
       <dss file="output/ras.dss" pn="/HSE/CELL161/PONDING//1DAY/CALC/">
</dss>
    </cellmonitor>
    <cellmonitor id="224" attr="ponding">
       <dss file="output/ras.dss" pn="/HSE/CELL224/PONDING//1DAY/CALC/">
</dss>
    </cellmonitor>
    <cellmonitor id="225" attr="ponding">
       <dss file="output/ras.dss" pn="/HSE/CELL225/PONDING//1DAY/CALC/">
</dss>
    </cellmonitor>
    <cellmonitor id="369" attr="ponding">
       <dss file="output/ras.dss" pn="/HSE/CELL369/PONDING//1DAY/CALC/">
</dss>
    </cellmonitor>
    <cellmonitor id="370" attr="ponding">
       <dss file="output/ras.dss" pn="/HSE/CELL370/PONDING//1DAY/CALC/">
</dss>
    </cellmonitor>
    <cellmonitor id="422" attr="ponding">
       <dss file="output/ras.dss" pn="/HSE/CELL422/PONDING//1DAY/CALC/">
</dss>
    </cellmonitor>
    <cellmonitor id="455" attr="ponding">
       <dss file="output/ras.dss" pn="/HSE/CELL455/PONDING//1DAY/CALC/">
</dss>
    </cellmonitor>
    <cellmonitor id="227" attr="ponding">
       <dss file="output/ras.dss" pn="/HSE/CELL227/PONDING//1DAY/CALC/">
</dss>
    </cellmonitor>
    <cellmonitor id="228" attr="ponding">
       <dss file="output/ras.dss" pn="/HSE/CELL228/PONDING//1DAY/CALC/">
```

```
</dss>
    </cellmonitor>
    <cellmonitor id="270" attr="ponding">
       <dss file="output/ras.dss" pn="/HSE/CELL270/PONDING//1DAY/CALC/">
</dss>
    </cellmonitor>
    <cellmonitor id="271" attr="ponding">
       <dss file="output/ras.dss" pn="/HSE/CELL271/PONDING//1DAY/CALC/">
</dss>
    </cellmonitor>
    <cellmonitor id="417" attr="ponding">
       <dss file="output/ras.dss" pn="/HSE/CELL417/PONDING//1DAY/CALC/">
</dss>
    </cellmonitor>
    <cellmonitor id="453" attr="ponding">
       <dss file="output/ras.dss" pn="/HSE/CELL453/PONDING//1DAY/CALC/">
</dss>
    </cellmonitor>
    <cellmonitor id="794" attr="head">
       <dss file="output/ras.dss" pn="/HSE/CELL794/HEAD//1DAY/CALC/"> </dss>
    </cellmonitor> -->
    <flowgage section="ol" label="39_41">
      <nodelist>39 41</nodelist>
      <dss file="output/ras.dss" pn="/HSE/FLOW_39_41/FLOW//1DAY/CALC/">
</dss>
    </flowgage>
    <flowgage section="ol" label="41_54">
      <nodelist>41 54</nodelist>
      <dss file="output/ras.dss" pn="/HSE/FLOW_41_54/FLOW//1DAY/CALC/">
</dss>
    </flowgage>
    <flowgage section="ol" label="54_68">
      <nodelist>54 68</nodelist>
      <dss file="output/ras.dss" pn="/HSE/FLOW_54_68/FLOW//1DAY/CALC/">
</dss>
    </flowgage>
    <flowgage section="ol" label="68_86">
      <nodelist>68 86</nodelist>
      <dss file="output/ras.dss" pn="/HSE/FLOW_68_86/FLOW//1DAY/CALC/">
</dss>
    </flowgage>
    <flowgage section="ol" label="78_97">
      <nodelist>78 97</nodelist>
      <dss file="output/ras.dss" pn="/HSE/FLOW_78_97/FLOW//1DAY/CALC/">
</dss>
    </flowgage>
    <flowgage section="ol" label="97_81">
      <nodelist>97 81</nodelist>
      <dss file="output/ras.dss" pn="/HSE/FLOW_97_81/FLOW//1DAY/CALC/">
</dss>
    </flowgage>
    <flowgage section="ol" label="81_82">
      <nodelist>81 82</nodelist>
      <dss file="output/ras.dss" pn="/HSE/FLOW_81_82/FLOW//1DAY/CALC/">
</dss>
    </flowgage>
    <flowgage section="ol" label="82_101">
```

```
      <nodelist>82 101</nodelist>
      <dss file="output/ras.dss" pn="/HSE/FLOW_82_101/FLOW//1DAY/CALC/">
</dss>
    </flowgage>
    <flowgage section="ol" label="101_120">
      <nodelist>101 120</nodelist>
      <dss file="output/ras.dss" pn="/HSE/FLOW_101_120/FLOW//1DAY/CALC/">
</dss>
    </flowgage>
    <flowgage section="ol" label="54_67">
      <nodelist>54 67</nodelist>
      <dss file="output/ras.dss" pn="/HSE/FLOW_54_67/FLOW//1DAY/CALC/">
</dss>
    </flowgage>
    <flowgage section="ol" label="53_54">
      <nodelist>53 54</nodelist>
      <dss file="output/ras.dss" pn="/HSE/FLOW_53_54/FLOW//1DAY/CALC/">
</dss>
    </flowgage>
    <flowgage section="ol" label="53_67">
      <nodelist>53 67</nodelist>
      <dss file="output/ras.dss" pn="/HSE/FLOW_53_67/FLOW//1DAY/CALC/">
</dss>
    </flowgage>
    <flowgage section="ol" label="43_56">
      <nodelist>43 56</nodelist>
      <dss file="output/ras.dss" pn="/HSE/FLOW_43_56/FLOW//1DAY/CALC/">
</dss>
    </flowgage>
    <flowgage section="ol" label="42_43">
      <nodelist>42 43</nodelist>
      <dss file="output/ras.dss" pn="/HSE/FLOW_42_43/FLOW//1DAY/CALC/">
</dss>
    </flowgage>
    <flowgage section="ol" label="42_56">
      <nodelist>42 56</nodelist>
      <dss file="output/ras.dss" pn="/HSE/FLOW_42_56/FLOW//1DAY/CALC/">
</dss>
    </flowgage>
    <flowgage section="ol" label="41_53">
      <nodelist>41 53</nodelist>
      <dss file="output/ras.dss" pn="/HSE/FLOW_41_53/FLOW//1DAY/CALC/">
</dss>
    </flowgage>
    <flowgage section="ol" label="67_68">
      <nodelist>67 68</nodelist>
      <dss file="output/ras.dss" pn="/HSE/FLOW_67_68/FLOW//1DAY/CALC/">
</dss>
    </flowgage>
    <flowgage section="ol" label="81_98">
      <nodelist>81 98</nodelist>
      <dss file="output/ras.dss" pn="/HSE/FLOW_81_98/FLOW//1DAY/CALC/">
</dss>
    </flowgage>
    <flowgage section="ol" label="82_100">
      <nodelist>82 100</nodelist>
      <dss file="output/ras.dss" pn="/HSE/FLOW_82_100/FLOW//1DAY/CALC/">
```

```
</dss>
    </flowgage>
    <flowgage section="ol" label="99_116">
      <nodelist>99 116</nodelist>
      <dss file="output/ras.dss" pn="/HSE/FLOW_99_116/FLOW//1DAY/CALC/">
</dss>
    </flowgage>
    <flowgage section="ol" label="99_117">
      <nodelist>99 117</nodelist>
      <dss file="output/ras.dss" pn="/HSE/FLOW_99_117/FLOW//1DAY/CALC/">
</dss>
    </flowgage>
    <flowgage section="ol" label="81_99">
      <nodelist>81 99</nodelist>
      <dss file="output/ras.dss" pn="/HSE/FLOW_81_99/FLOW//1DAY/CALC/">
</dss>
    </flowgage>
    <flowgage section="ol" label="98_99">
      <nodelist>98 99</nodelist>
      <dss file="output/ras.dss" pn="/HSE/FLOW_98_99/FLOW//1DAY/CALC/">
</dss>
    </flowgage>
    <flowgage section="ol" label="99_100">
      <nodelist>99 100</nodelist>
      <dss file="output/ras.dss" pn="/HSE/FLOW_99_100/FLOW//1DAY/CALC/">
</dss>
    </flowgage>
    <flowgage section="ol" label="99_82">
      <nodelist>99 82</nodelist>
      <dss file="output/ras.dss" pn="/HSE/FLOW_99_82/FLOW//1DAY/CALC/">
</dss>
    </flowgage>
    <flowgage section="ol" label="98_116">
      <nodelist>98 116</nodelist>
      <dss file="output/ras.dss" pn="/HSE/FLOW_98_116/FLOW//1DAY/CALC/">
</dss>
    </flowgage>
    <flowgage section="ol" label="66_67">
      <nodelist>66 67</nodelist>
      <dss file="output/ras.dss" pn="/HSE/FLOW_66_67/FLOW//1DAY/CALC/">
</dss>
    </flowgage>
    <flowgage section="ol" label="66_83">
      <nodelist>66 83</nodelist>
      <dss file="output/ras.dss" pn="/HSE/FLOW_66_83/FLOW//1DAY/CALC/">
</dss>
    </flowgage>
    <flowgage section="ol" label="67_83">
      <nodelist>67 83</nodelist>
      <dss file="output/ras.dss" pn="/HSE/FLOW_67_83/FLOW//1DAY/CALC/">
</dss>
    </flowgage>
    <flowgage section="ol" label="116_117">
      <nodelist>116 117</nodelist>
      <dss file="output/ras.dss" pn="/HSE/FLOW_116_117/FLOW//1DAY/CALC/">
</dss>
    </flowgage>
```

```
    <flowgage section="ol" label="100_117">
      <nodelist>100 117</nodelist>
      <dss file="output/ras.dss" pn="/HSE/FLOW_100_117/FLOW//1DAY/CALC/">
</dss>
    </flowgage>
    <flowgage section="ol" label="42_43">
      <nodelist>42 43</nodelist>
      <asciiform file="output/flow_42_43.dat" format="%lf"/>
    </flowgage>
    <flowgage section="ol" label="42_56">
      <nodelist>42 56</nodelist>
      <asciiform file="output/flow_42_56.dat" format="%lf"/>
    </flowgage>
    <flowgage section="ol" label="39_41">
      <nodelist>39 41</nodelist>
      <asciiform file="output/flow_39_41.dat" format="%lf"/>
    </flowgage>
    <flowgage section="ol" label="41_54">
      <nodelist>41 54</nodelist>
      <asciiform file="output/flow_41_54.dat" format="%lf"/>
    </flowgage>
    <flowgage section="ol" label="54_68">
      <nodelist>54 68</nodelist>
      <asciiform file="output/flow_54_68.dat" format="%lf"/>
    </flowgage>
    <flowgage section="ol" label="68_86">
      <nodelist>68 86</nodelist>
      <asciiform file="output/flow_68_86.dat" format="%lf"/>
    </flowgage>
    <flowgage section="ol" label="78_97">
      <nodelist>78 97</nodelist>
      <asciiform file="output/flow_78_97.dat" format="%lf"/>
    </flowgage>
    <flowgage section="ol" label="97_81">
      <nodelist>97 81</nodelist>
      <asciiform file="output/flow_97_81.dat" format="%lf"/>
    </flowgage>
    <flowgage section="ol" label="81_82">
      <nodelist>81 82</nodelist>
      <asciiform file="output/flow_81_82.dat" format="%lf"/>
    </flowgage>
    <flowgage section="ol" label="82_101">
      <nodelist>82 101</nodelist>
      <asciiform file="output/flow_82_101.dat" format="%lf"/>
    </flowgage>
    <flowgage section="ol" label="101_120">
      <nodelist>101 120</nodelist>
      <asciiform file="output/flow_101_120.dat" format="%lf"/>
    </flowgage>
    <flowgage section="ol" label="41_53">
      <nodelist>41 53</nodelist>
      <asciiform file="output/flow_41_53.dat" format="%lf"/>
    </flowgage>
    <flowgage section="ol" label="67_68">
      <nodelist>67 68</nodelist>
      <asciiform file="output/flow_67_68.dat" format="%lf"/>
    </flowgage>
```

```
    <flowgage section="ol" label="81_98">
      <nodelist>81 98</nodelist>
      <asciiform file="output/flow_81_98.dat" format="%lf"/>
    </flowgage>
    <flowgage section="ol" label="82_100">
      <nodelist>82 100</nodelist>
      <asciiform file="output/flow_82_100.dat" format="%lf"/>
    </flowgage>
    <flowgage section="ol" label="99_116">
      <nodelist>99 116</nodelist>
      <asciiform file="output/flow_99_116.dat" format="%lf"/>
    </flowgage>
    <flowgage section="ol" label="99_117">
      <nodelist>99 117</nodelist>
      <asciiform file="output/flow_99_117.dat" format="%lf"/>
    </flowgage>
    <globalmonitor attr="totalvector">
       <gms file="output/outvect.dat"> </gms>
    </globalmonitor>
  </output>
</hse>
```

Appendix D. Dry season transport model under current flow regime (RSM TaRSE) xml input file


```
<?xml version="1.0" ?>
<!DOCTYPE wq SYSTEM "./equations.dtd" [ ]>
<wq version="0.1">
  <control
    tslen="10"
    tstype="minute"
    use_operator_splitting="true"
    postprocess="false"
    linear_solver_type="cg"
    linear_preconditioner_type="ilu"
    chemistry_solver_type="gmres"
    chemistry_preconditioner_type="ilu"
    implicit_weighting="1.0"
    max_cfl="0.33"
    slope_estimator="none"
    limiter_type="none"
    fixed_velocity="false">

  <chemistry_solver order="2">runge_kutta</chemistry_solver>
  </control>
  <stores>
    <store full_name="Surface Water" coverage="global"
distribution="heterogeneous" location="element" section="ol"
actuator="rsm_wm">
      <name>surface_water</name>
      <components>
        <variables>
          <variable type="mobile">
            <name full_name="TSSwc">TSSwc</name>
            <initial_distribution type="constant">0.0</initial_distribution>
          </variable>
          <variable type="stabile">
            <name full_name="TSSdep">TSSdep</name>
            <initial_distribution type="constant">0.0</initial_distribution>
          </variable>
        </variables>
        <parameters>
          <parameter units="meter">
            <name>longitudinal_dispersivity</name>
            <initial_distribution type="constant">20.0</initial_distribution>
          </parameter>
          <parameter units="meter">
            <name>transverse_dispersivity</name>
            <initial_distribution type="constant">2.0</initial_distribution>
          </parameter>
          <parameter units="none">
            <name>k_st</name>
            <initial_distribution type="constant">0.0</initial_distribution>
          </parameter>
          <parameter units="none">
            <name>k_rs</name>
            <initial_distribution type="constant">0.0</initial_distribution>
          </parameter>
```

```
          <parameter units="meter">
            <name>molecular_diffusion</name>
            <initial_distribution type="constant">0.0</initial_distribution>
          </parameter>
          <parameter units="none">
            <name>surface_porosity</name>
            <initial_distribution type="constant">1.0</initial_distribution>
          </parameter>
          <parameter units="none">
            <name>soil_porosity</name>
            <initial_distribution type="constant">0.3</initial_distribution>
          </parameter>
          <parameter  units="meter">
            <name>active_soil_depth</name>
            <initial_distribution type="constant">0.1</initial_distribution>
          </parameter>
          <parameter  units="none">
            <name>fraction_organic_soil</name>
            <initial_distribution type="constant">0.00</initial_distribution>
          </parameter>
          <parameter units="none">
            <name>fraction_inorganic_soil</name>
            <initial_distribution type="constant">0.00</initial_distribution>
          </parameter>
          <parameter  units="none">
            <name>bulk_density</name>
            <initial_distribution type="constant">0.4</initial_distribution>
          </parameter>
        </parameters>
      </components>
    </store>
  </stores>
<mesh>
      <source section="ol" cell_id="86" store_name="surface_water"
      actuator="rsm_source_flow" actuator_name="Well1">
        <variable>
          <name>TSSwc</name>
          <data type="non_constant"
format="gwq_time_series">Imag_tracer_dry.dat</data>
        </variable>
      </source>
</mesh>

<equations use="true">
    <equation>
      <lhs>TSSwc</lhs>
      <rhs>-k_st*TSSwc + k_rs*TSSdep/depth</rhs>
    </equation>
    <equation>
      <lhs>TSSdep</lhs>
      <rhs>depth*k_st*TSSwc - k_rs*TSSdep</rhs>
    </equation>
</equations>
  <output>
    <monitor type="edge" id="42 43">
      <for>TSSwc</for>
      <destination type="text" every="6" delimiter="," time_format="%Y-%b-
```

%d:%H:%M">./output/concbnd_42_43.dat</destination>
    </monitor>
    <monitor type="edge" id="42 56">
      <for>TSSwc</for>
      <destination type="text" every="6" delimiter="," time_format="%Y-%b-
%d:%H:%M">./output/concbnd_42_56.dat</destination>
    </monitor>
    <monitor type="edge" id="43 56">
      <for>TSSwc</for>
      <destination type="text" every="6" delimiter="," time_format="%Y-%b-
%d:%H:%M">./output/concbnd_43_56.dat</destination>
    </monitor>
    <monitor type="edge" id="39 41">
      <for>TSSwc</for>
      <destination type="text" every="6" delimiter="," time_format="%Y-%b-
%d:%H:%M">./output/concbnd_39_41.dat</destination>
    </monitor>
    <monitor type="edge" id="41 54">
      <for>TSSwc</for>
      <destination type="text" every="6" delimiter="," time_format="%Y-%b-
%d:%H:%M">./output/concbnd_41_54.dat</destination>
    </monitor>
    <monitor type="edge" id="54 68">
      <for>TSSwc</for>
      <destination type="text" every="6" delimiter="," time_format="%Y-%b-
%d:%H:%M">./output/concbnd_54_68.dat</destination>
    </monitor>
    <monitor type="edge" id="68 86">
      <for>TSSwc</for>
      <destination type="text" every="6" delimiter="," time_format="%Y-%b-
%d:%H:%M">./output/concbnd_68_86.dat</destination>
    </monitor>
    <monitor type="edge" id="78 97">
      <for>TSSwc</for>
      <destination type="text" every="6" delimiter="," time_format="%Y-%b-
%d:%H:%M">./output/concbnd_78_97.dat</destination>
    </monitor>
    <monitor type="edge" id="97 81">
      <for>TSSwc</for>
      <destination type="text" every="6" delimiter="," time_format="%Y-%b-
%d:%H:%M">./output/concbnd_97_81.dat</destination>
    </monitor>
    <monitor type="edge" id="81 82">
      <for>TSSwc</for>
      <destination type="text" every="6" delimiter="," time_format="%Y-%b-
%d:%H:%M">./output/concbnd_81_82.dat</destination>
    </monitor>
    <monitor type="edge" id="82 101">
      <for>TSSwc</for>
      <destination type="text" every="6" delimiter="," time_format="%Y-%b-
%d:%H:%M">./output/concbnd_82_101.dat</destination>
    </monitor>
    <monitor type="edge" id="101 120">
      <for>TSSwc</for>
      <destination type="text" every="6" delimiter="," time_format="%Y-%b-
%d:%H:%M">./output/concbnd_101_120.dat</destination>
    </monitor>

```
    <monitor type="edge" id="41 53">
      <for>TSSwc</for>
      <destination type="text" every="6" delimiter="," time_format="%Y-%b-
%d:%H:%M">./output/concbnd_41_53.dat</destination>
    </monitor>
    <monitor type="edge" id="67 68">
      <for>TSSwc</for>
      <destination type="text" every="6" delimiter="," time_format="%Y-%b-
%d:%H:%M">./output/concbnd_67_68.dat</destination>
    </monitor>
    <monitor type="edge" id="81 98">
      <for>TSSwc</for>
      <destination type="text" every="6" delimiter="," time_format="%Y-%b-
%d:%H:%M">./output/concbnd_81_98.dat</destination>
    </monitor>
    <monitor type="edge" id="82 100">
      <for>TSSwc</for>
      <destination type="text" every="6" delimiter="," time_format="%Y-%b-
%d:%H:%M">./output/concbnd_82_100.dat</destination>
    </monitor>
    <monitor type="edge" id="99 116">
      <for>TSSwc</for>
      <destination type="text" every="6" delimiter="," time_format="%Y-%b-
%d:%H:%M">./output/concbnd_99_116.dat</destination>
    </monitor>
    <monitor type="edge" id="99 117">
      <for>TSSwc</for>
      <destination type="text" every="6" delimiter="," time_format="%Y-%b-
%d:%H:%M">./output/concbnd_99_117.dat</destination>
    </monitor>
    <monitor type="edge" id="54 67">
      <for>TSSwc</for>
      <destination type="text" every="6" delimiter="," time_format="%Y-%b-
%d:%H:%M">./output/concbnd_54_67.dat</destination>
    </monitor>
    <monitor type="edge" id="53 54">
      <for>TSSwc</for>
      <destination type="text" every="6" delimiter="," time_format="%Y-%b-
%d:%H:%M">./output/concbnd_53_54.dat</destination>
    </monitor>
    <monitor type="edge" id="53 67">
      <for>TSSwc</for>
      <destination type="text" every="6" delimiter="," time_format="%Y-%b-
%d:%H:%M">./output/concbnd_53_67.dat</destination>
    </monitor>
    <monitor type="edge" id="81 99">
      <for>TSSwc</for>
      <destination type="text" every="6" delimiter="," time_format="%Y-%b-
%d:%H:%M">./output/concbnd_81_99.dat</destination>
    </monitor>
    <monitor type="edge" id="99 82">
      <for>TSSwc</for>
      <destination type="text" every="6" delimiter="," time_format="%Y-%b-
%d:%H:%M">./output/concbnd_99_82.dat</destination>
    </monitor>
    <monitor type="edge" id="98 99">
      <for>TSSwc</for>
```

```
      <destination type="text" every="6" delimiter="," time_format="%Y-%b-
%d:%H:%M">./output/concbnd_98_99.dat</destination>
    </monitor>
    <monitor type="edge" id="99 100">
      <for>TSSwc</for>
      <destination type="text" every="6" delimiter="," time_format="%Y-%b-
%d:%H:%M">./output/concbnd_99_100.dat</destination>
    </monitor>
    <monitor type="cell" id="86">
      <for>TSSwc</for>
      <for>area</for>
      <for>depth</for>
      <for>vel_mag_ol</for>
      <for>x_vel_ol</for>
      <for>y_vel_ol</for>
      <destination type="text" every="6" time_format="%Y-%b-
%d:%H:%M">./output/cell86_out.dat</destination>
    </monitor>
    <monitor type="cell" id="78">
      <for>TSSwc</for>
      <for>area</for>
      <for>depth</for>
      <for>vel_mag_ol</for>
      <for>x_vel_ol</for>
      <for>y_vel_ol</for>
      <destination type="text" every="6" time_format="%Y-%b-
%d:%H:%M">./output/cell78_out.dat</destination>
    </monitor>
    <monitor type="cell" id="79">
      <for>TSSwc</for>
      <for>area</for>
      <for>depth</for>
      <for>vel_mag_ol</for>
      <for>x_vel_ol</for>
      <for>y_vel_ol</for>
      <destination type="text" every="6" time_format="%Y-%b-
%d:%H:%M">./output/cell79_out.dat</destination>
    </monitor>
    <monitor type="cell" id="81">
      <for>TSSwc</for>
      <for>area</for>
      <for>depth</for>
      <for>vel_mag_ol</for>
      <for>x_vel_ol</for>
      <for>y_vel_ol</for>
      <destination type="text" every="6" time_format="%Y-%b-
%d:%H:%M">./output/cell81_out.dat</destination>
    </monitor>
    <monitor type="cell" id="82">
      <for>TSSwc</for>
      <for>area</for>
      <for>depth</for>
      <for>vel_mag_ol</for>
      <for>x_vel_ol</for>
      <for>y_vel_ol</for>
      <destination type="text" every="6" time_format="%Y-%b-
%d:%H:%M">./output/cell82_out.dat</destination>
```

```
    </monitor>
    <monitor type="cell" id="106">
      <for>TSSwc</for>
      <for>area</for>
      <for>depth</for>
      <for>vel_mag_ol</for>
      <for>x_vel_ol</for>
      <for>y_vel_ol</for>
      <destination type="text" every="6" time_format="%Y-%b-
%d:%H:%M">./output/cell106_out.dat</destination>
    </monitor>
    <monitor type="cell" id="107">
      <for>TSSwc</for>
      <for>area</for>
      <for>depth</for>
      <for>vel_mag_ol</for>
      <for>x_vel_ol</for>
      <for>y_vel_ol</for>
      <destination type="text" every="6" time_format="%Y-%b-
%d:%H:%M">./output/cell107_out.dat</destination>
    </monitor>
    <monitor type="cell" id="136">
      <for>TSSwc</for>
      <for>area</for>
      <for>depth</for>
      <for>vel_mag_ol</for>
      <for>x_vel_ol</for>
      <for>y_vel_ol</for>
      <destination type="text" every="6" time_format="%Y-%b-
%d:%H:%M">./output/cell136_out.dat</destination>
    </monitor>
    <monitor type="cell" id="137">
      <for>TSSwc</for>
      <for>area</for>
      <for>depth</for>
      <for>vel_mag_ol</for>
      <for>x_vel_ol</for>
      <for>y_vel_ol</for>
      <destination type="text" every="6" time_format="%Y-%b-
%d:%H:%M">./output/cell137_out.dat</destination>
    </monitor>
    <monitor type="cell" id="170">
      <for>TSSwc</for>
      <for>area</for>
      <for>depth</for>
      <for>vel_mag_ol</for>
      <for>x_vel_ol</for>
      <for>y_vel_ol</for>
      <destination type="text" every="6" time_format="%Y-%b-
%d:%H:%M">./output/cell170_out.dat</destination>
    </monitor>
    <monitor type="cell" id="155">
      <for>TSSwc</for>
      <for>area</for>
      <for>depth</for>
      <for>vel_mag_ol</for>
      <for>x_vel_ol</for>
```

```
      <for>y_vel_ol</for>
      <destination type="text" every="6" time_format="%Y-%b-
%d:%H:%M">./output/cell155_out.dat</destination>
    </monitor>
    <monitor type="cell" id="156">
      <for>TSSwc</for>
      <for>area</for>
      <for>depth</for>
      <for>vel_mag_ol</for>
      <for>x_vel_ol</for>
      <for>y_vel_ol</for>
      <destination type="text" every="6" time_format="%Y-%b-
%d:%H:%M">./output/cell156_out.dat</destination>
    </monitor>
    <monitor type="cell" id="192">
      <for>TSSwc</for>
      <for>area</for>
      <for>depth</for>
      <for>vel_mag_ol</for>
      <for>x_vel_ol</for>
      <for>y_vel_ol</for>
      <destination type="text" every="6" time_format="%Y-%b-
%d:%H:%M">./output/cell192_out.dat</destination>
    </monitor>
    <monitor type="cell" id="160">
      <for>TSSwc</for>
      <for>area</for>
      <for>depth</for>
      <for>vel_mag_ol</for>
      <for>x_vel_ol</for>
      <for>y_vel_ol</for>
      <destination type="text" every="6" time_format="%Y-%b-
%d:%H:%M">./output/cell160_out.dat</destination>
    </monitor>
    <monitor type="cell" id="161">
      <for>TSSwc</for>
      <for>area</for>
      <for>depth</for>
      <for>vel_mag_ol</for>
      <for>x_vel_ol</for>
      <for>y_vel_ol</for>
      <destination type="text" every="6" time_format="%Y-%b-
%d:%H:%M">./output/cell161_out.dat</destination>
    </monitor>
    <monitor type="cell" id="162">
      <for>TSSwc</for>
      <for>area</for>
      <for>depth</for>
      <for>vel_mag_ol</for>
      <for>x_vel_ol</for>
      <for>y_vel_ol</for>
      <destination type="text" every="6" time_format="%Y-%b-
%d:%H:%M">./output/cell162_out.dat</destination>
    </monitor>
    <monitor type="cell" id="163">
      <for>TSSwc</for>
      <for>area</for>
```

```
      <for>depth</for>
      <for>vel_mag_ol</for>
      <for>x_vel_ol</for>
      <for>y_vel_ol</for>
      <destination type="text" every="6" time_format="%Y-%b-
%d:%H:%M">./output/cell163_out.dat</destination>
    </monitor>
    <monitor type="cell" id="164">
      <for>TSSwc</for>
      <for>area</for>
      <for>depth</for>
      <for>vel_mag_ol</for>
      <for>x_vel_ol</for>
      <for>y_vel_ol</for>
      <destination type="text" every="6" time_format="%Y-%b-
%d:%H:%M">./output/cell164_out.dat</destination>
    </monitor>
    <monitor type="cell" id="199">
      <for>TSSwc</for>
      <for>area</for>
      <for>depth</for>
      <for>vel_mag_ol</for>
      <for>x_vel_ol</for>
      <for>y_vel_ol</for>
      <destination type="text" every="6" time_format="%Y-%b-
%d:%H:%M">./output/cell199_out.dat</destination>
    </monitor>
    <monitor type="cell" id="200">
      <for>TSSwc</for>
      <for>area</for>
      <for>depth</for>
      <for>vel_mag_ol</for>
      <for>x_vel_ol</for>
      <for>y_vel_ol</for>
      <destination type="text" every="6" time_format="%Y-%b-
%d:%H:%M">./output/cell200_out.dat</destination>
    </monitor>
    <monitor type="cell" id="83">
      <for>TSSwc</for>
      <for>area</for>
      <for>depth</for>
      <for>vel_mag_ol</for>
      <for>x_vel_ol</for>
      <for>y_vel_ol</for>
      <destination type="text" every="6" time_format="%Y-%b-
%d:%H:%M">./output/cell83_out.dat</destination>
    </monitor>
    <monitor type="cell" id="108">
      <for>TSSwc</for>
      <for>area</for>
      <for>depth</for>
      <for>vel_mag_ol</for>
      <for>x_vel_ol</for>
      <for>y_vel_ol</for>
      <destination type="text" every="6" time_format="%Y-%b-
%d:%H:%M">./output/cell108_out.dat</destination>
    </monitor>
```

```
    <monitor type="cell" id="194">
      <for>TSSwc</for>
      <for>area</for>
      <for>depth</for>
      <for>vel_mag_ol</for>
      <for>x_vel_ol</for>
      <for>y_vel_ol</for>
      <destination type="text" every="6" time_format="%Y-%b-
%d:%H:%M">./output/cell194_out.dat</destination>
    </monitor>
    <monitor type="cell" id="195">
      <for>TSSwc</for>
      <for>area</for>
      <for>depth</for>
      <for>vel_mag_ol</for>
      <for>x_vel_ol</for>
      <for>y_vel_ol</for>
      <destination type="text" every="6" time_format="%Y-%b-
%d:%H:%M">./output/cell195_out.dat</destination>
    </monitor>
    <monitor type="cell" id="105">
      <for>TSSwc</for>
      <for>area</for>
      <for>depth</for>
      <for>vel_mag_ol</for>
      <for>x_vel_ol</for>
      <for>y_vel_ol</for>
      <destination type="text" every="6" time_format="%Y-%b-
%d:%H:%M">./output/cell105_out.dat</destination>
    </monitor>
    <monitor type="cell" id="133">
      <for>TSSwc</for>
      <for>area</for>
      <for>depth</for>
      <for>vel_mag_ol</for>
      <for>x_vel_ol</for>
      <for>y_vel_ol</for>
      <destination type="text" every="6" time_format="%Y-%b-
%d:%H:%M">./output/cell133_out.dat</destination>
    </monitor>
    <monitor type="cell" id="132">
      <for>TSSwc</for>
      <for>area</for>
      <for>depth</for>
      <for>vel_mag_ol</for>
      <for>x_vel_ol</for>
      <for>y_vel_ol</for>
      <destination type="text" every="6" time_format="%Y-%b-
%d:%H:%M">./output/cell132_out.dat</destination>
    </monitor>
    <monitor type="cell" id="196">
      <for>TSSwc</for>
      <for>area</for>
      <for>depth</for>
      <for>vel_mag_ol</for>
      <for>x_vel_ol</for>
      <for>y_vel_ol</for>
```

```
      <destination type="text" every="6" time_format="%Y-%b-
%d:%H:%M">./output/cell196_out.dat</destination>
    </monitor>
    <monitor type="global">
      <for>TSSwc</for>
      <for>area</for>
      <for>depth</for>
      <for>vel_mag_ol</for>
      <for>x_vel_ol</for>
      <for>y_vel_ol</for>
      <destination type="text" every="6" delimiter="," time_format="%Y-%b-
%d:%H:%M">./output/text_output.dat</destination>
    </monitor>
    <monitor type="global">
      <for>TSSwc</for>
      <for>area</for>
      <for>depth</for>
      <for>vel_mag_ol</for>
      <for>x_vel_ol</for>
      <for>y_vel_ol</for>
      <destination type="tecplot" every="18" time_format="%Y-%b-
%d:%H:%M">./output/TecOutput.dat</destination>
    </monitor>
  </output>
</wq>
```